26

Electrotherapy on Cancer: Experiment and Mathematical Modeling

Ana Elisa Bergues Pupo[1], Rolando Placeres Jiménez[2] and Luis Enrique Bergues Cabrales[3]

[1]*Universidad de Oriente, Facultad de Ciencias Naturales y Matemáticas, Departamento de Física, Patricio Lumumba s/n, Santiago de Cuba*

[2]*Departamento de Física, Universidade Federal São Carlos, São Carlos-SP,*

[3]*Universidad de Oriente, Centro Nacional de Electromagnetismo Aplicado, Departamento de Investigaciones, Ave. Las Américas s/n, Santiago de Cuba*

[1,3]*Cuba*

[2]*Brasil*

1. Introduction

In this chapter are discussed the use, antitumor mechanisms and potentialities of electrotherapy of low-level direct current in cancer. We make emphasis in one of the most stimulating problems in the theme of electrotherapy-cancer as is the propose of electrode arrays that efficiently distribute the electric current density (electric field) in the tumor and its surrounding healthy tissue in order to maximize the tumor destruction with the minimum damage to the organism. A mathematical theorem is intended to obtain the analytical expressions for three-dimensional electric current density (electric field) generated by arrays of electrodes with finite length from those obtained for a point electrodes array. The importance and application of these electrode arrays in therapeutic planning are also discussed.

Electrotherapy is based on principles developed during the nineteenth and twentieth centuries following the first demonstration of "animal electricity" by Luigi Galvani in the eighteenth century. In medicine, the term electrotherapy has been applied to a range of alternative medical devices and treatments. Reputable medical and therapy Journals report that the use of electrotherapy devices has been widely researched and the advantages have been well accepted in the field of rehabilitation and in the treatment of chronic wounds, pressure ulcers, pain (improves range of joint movement) and neuromuscular dysfunction (improvement of strength, improvement of motor control, retards muscle atrophy and improves local blood flow). Also, electrotherapy has been applied in tissue repair (enhances microcirculation and protein synthesis to heal wounds and restores integrity of connective and dermal tissues), acute and chronic edema (accelerates absorption rate, affects blood vessel permeability, and increases mobility of proteins, blood cells and lymphatic flow), peripheral blood flow (induces arterial, venous and lymphatic flow), iontophoresis (delivery of pharmacological agents), urine and fecal incontinence (affects pelvic floor musculature to reduce pelvic pain and strengthen musculature and treatment may lead to complete

continence). Yet some of the treatment effectiveness mechanisms are little understood. Therefore effectiveness and best practices for their use in some instances are still anecdotal [Joa, 2010].

On the other hand, the application of electrotherapy in cancerous tissue has been found to have a beneficial effect in some cases of cancer. Many different forms of electrical current with respect to frequencies, pulse-shapes and amplitudes have been employed in biomedicine with the aim of remodeling tissues by enhancing or suppressing cell proliferation. One of the scopes is also employment of direct current as an antitumor agent [Cabrales et al., 2001; Ciria et al., 2004; Jarque et al., 2007; Ren et al., 2001; Schaefer et al., 2008; Turler, et al., 2000; Vodovnik et al., 1992; Xin et al., 2004; Yoon et al., 2007].

2. Electrotherapy on cancer

Cancer is uncontrolled cell growth and its cause is not well understood. The tumor cells are aggressive (grow and divide without respect to normal limits), invasive (invade and destroy adjacent tissues) and metastatic (spread to other locations in the body) [Cohen & Arnold, 2008]. These malignant properties of cancer differentiate of the benign tumors, which are self-limited in the growth and do not invade or metastasize.

Tumor cells have some structural and physiological characteristics that reveal their electric properties, which differ from the ones of the surrounding healthy cells. One of these properties is a smaller transmembrane potential, which happens due to the fact that sodium and water present an inward flow, while potassium, zinc, calcium and magnesium flow outwards. Another of these properties is the accumulation of an excessive amount of negative charges in the outer area, which causes the reduction of intracellular potassium and the increase of intracellular sodium that lead to a carcinogenic state in the cell. Other characteristics are the electric field decrease through the membrane, a greater electrical conductivity and permittivity, the existence of abnormal electron-transference systems, the negative bioelectrical potentials, the alteration of the normal energy production process which uses electron transport and the hydrogen ion gradient through the mitochondrial membrane, and finally, the existence of areas with a relative electron deficit [Haltiwanger, 2008; Joa, 2010].

Surgery, chemotherapy, radiation therapy, immunotherapy (vaccines, monoclonal antibody therapy, among other) are the conventional therapies for treating cancer [Haltiwanger, 2008; Vinageras et al., 2008; Xiang et al., 2008; Xin et al., 2004]. Choice of therapy depends upon tumor characteristics (location, histological variety, size and stage) and state of patient. However, these conventional therapies have major side effects, have no given a complete solution to the cancer problem, and are costly too. Hence attractive alternative, affordable, effective treatments are sought and one of the upcoming treatments is the use of electrical therapies, as electrochemotherapy [Sadadcharam et al., 2008] and electrotherapy [Cabrales et al., 2010]. The characteristics of tumor cells above mentioned may prevent the reparation and re-establishing of the normal metabolic functions of the tumor cell, but, on the other hand, they facilitate the anti-tumor action of the electrotherapy.

2.1 Preclinical and clinical studies

Electrotherapy consists in the application of a low-level direct current to the solid tumor by means of the electrodes (i.e., platinum, platinum-iridium 90/10, stainless steel). The needles are connected to an electrical device that produces a direct current, which is generated by an

applied voltage between two electrodes. The needles with a positive charge are named anodes, while the needles with a negative charge are the cathodes. Different shapes of needles are used for treatment of tumors in dependence of the size and constitution of the tumor type. Harder needles are used to treat superficial tumors (breast, skin, melanoma cancers) [Jarque et al., 2007; Xin et al., 2004] and more elastic needles are used to treat visceral tumors (lung, liver, esophageal, prostate and rectal cancers) [Chou et al., 1997; Vogl et al., 2007; Xin et al., 2004; Yoon et al., 2007]. The location of the tumor should be determined before treatment. It and the tumor size are determined by palpation with hand for the case of superficial tumors; however, in visceral tumors are determined by means of computer tomography, X ray, Imaging Nuclear Magnetic Resonance and/or ultrasound. Normally, the treatment with electrotherapy is carried out under local anesthetic and on an outpatient basis. The tumor size determines how many needle electrodes are required, which are introduced into the tumor through the skin.

Many physicians have successfully used electrotherapy, also known as electrochemical tumor therapy, Galvanotherapy and electro-cancer treatment, as a standalone treatment in thousands of cases, with some truly spectacular results. There are many potential advantages of electrotherapy over conventional treatments, such as: (1) Direct current is suitable for all types of superficial or visceral tumors, both malignant and benign. (2) This therapy is easy to perform, safe, effective, inexpensive, induces minimum damages to the organism, can be carried out on an out-patient basis and it can be applied when the conventional therapies fail or cannot be applied. (3) It may be best suitable for cancers near critical organs where surgery and/or radiation therapy have failed or could not be performed without damaging other normal parts. (4) This therapy not only reduces costs of chemotherapy, radiotherapy, hyperthermia and immunotherapy, but also improves compliance. (5) Electrotherapy may be suitable for nonresectable tumors and can save functional tissues [Jarque et al., 2007; Vogl et al., 2007; Xin et al., 2004; Yoon et al., 2007]. (6) The tumor and its surrounding healthy tissue have different electric and geometrical parameters [Aguilera et al., 2010; Cabrales et al., 2010; Foster, 2000; Foster & Schwan, 1996; Haemmerich et al., 2003; Haemmerich et al., 2009; Haltiwanger, 2008; Jiménez et al., 2011; Ng et al., 2008; Sekino et al., 2009; Seo et al., 2005; S.R. Smith et al., 1986; D.G. Smith et al., 2000], which enable electrically-mediated treatments to be more efficient for a given dose and the tumor tissue is more susceptible to damage from direct current than normal tissue, thus allowing the destruction of cancerous cells to occur when direct current is applied directly to the malignant tissue [Cabrales et al., 2001; Ciria et al., 2004; Jarque et al., 2007; Von Euler, 2003]. These are reasons for moving to direct current (electric field) method for treating cancer. Judging by the very positive therapy results, it can be assumed, that electrotherapy will become an important form of treatment for malignant diseases. In spite of these advantages, this therapy cannot be used on ascitic and hemolimphoyetic system tumors [Xin et al., 2004].

The first time that the insertion of electrodes in the base of the tumor significantly increases its destruction rate and decreases the damages to the body after the electrotherapy is published in 1997 [Chou et al., 1997]. Their report claims that this way of inserting the electrodes and alternating the sequence of cathodes and anodes induces a uniform electric field in the whole tumor, which causes a significant destruction of it. They also report that the ratio of the number of electrodes to the size of the tumor, taking into account the effective area with necrosis around the electrodes (2 cm). Since that research is conducted, most scientists have been using this type of data configuration.

Electrotherapy antitumor effectiveness can be enhanced when it is combined with intratumor injection of a chemostatic drug (i.e., bleomycin, cisplatin) [Jarque et al., 2007; Xin et al., 2004], saline solution [Jarque et al., 2007; Lin et al., 2000] and/or immunotherapy [Serša et al., 1990; Serša et al., 1992; Serša et al., 1994; Serša et al., 1996]. It has been demonstrated that intratumor bleomycin (cisplatin) treatment is more effective than intravenous treatment at the same dose and direct current potentiates the antitumor effectiveness of bleomycin several-fold [Xin et al., 2004].

In vitro and in vivo studies have demonstrated that an increase of direct current (voltage) intensity leads to an increase of electrotherapy antitumor effectiveness, as shown in Figure 1. This figure shows the Ehrlich tumor growth kinetics for the control group (CG) and different treated groups: TG1 (treated group with electrical charge of 6.7 mA for 45 min), TG2 (treated group with 11.7 mA for 45 min), and TG3 (treated group with 17 mA for 45 min). The minimum of the amount of volumetric electric charge required for the tumor destruction must be 35 coulombs/cm^3; however, high antitumor effectiveness is obtained when this physical magnitude is between 80 and 100 coulombs/cm^3 [Jarque et al., 2007; Ren et al., 2001; Xin et al., 2004; Yoon et al., 2007], in agreement with 92 and 80 coulombs/cm^3 for which the Ehrlich (TG3 in Figure 1) and fibrosarcoma Sa-37 tumors are completely destroyed, respectively [Ciria et al., 2004].

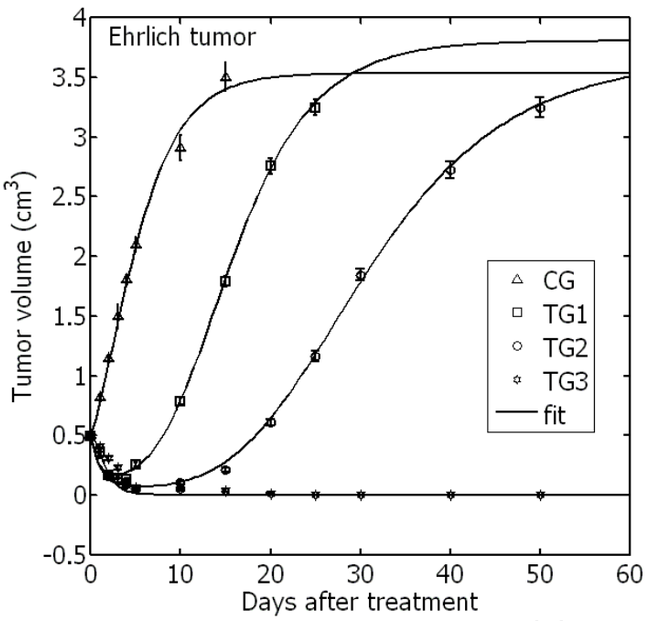

Fig. 1. Experimental data (mean ± standard deviation) and modeled growth curves of Ehrlich tumor. Each experimental group is formed by 10 mice. CG (control group), TG1 (treated group with electrical charge of 6.7 mA for 45 min), TG2 (treated group with 11.7 mA for 45 min), and TG3 (treated group with 17 mA for 45 min). When the tumors reached approximately 0.5 cm^3 in BALB/c mice, a single shot electrotherapy was supplied (zero day).

In 1978 the clinical use of direct current in the treatment of malignant tumors in humans is reported for the first time when Nordenström treated patients with lung cancer and explained that the anti-tumoral effects were due to the toxic products that came from the

electrochemical reactions induced on it because of the cytotoxic action of electrotherapy. Since Nordenström develops his work, the use of electrotherapy has been expanded for the treatment of patients with various histological types of cancer in other hospitals of Sweden and in different countries, as: China, Germany, Japan, Korea, Australia, Slovenia, the United States, Greece, Denmark, France, Brazil, Israel, Russia, Argentina and Cuba.

Since 1987 the electrotherapy has been used in China for the treatment of malignant and benign tumors, and so far it has been applied to over 20,000 patients. This is, therefore, the most complete clinical study to date. In the beginning, the group of researchers from China [Xin et al., 2004] changes the methodology for placing Nordenström's electrodes. Instead of placing one cathode in the tumor and one anode far from it, they insert several anodes in the center of the tumor and the same number of cathodes in the outer zone at the periphery of the tumor. Then, they modify again their electrode placing technique, and place the anodes and cathodes inside the tumor with the anodes in the center and the cathodes in the periphery. This change not only protects the normal tissue from destruction but also reinforce the effect of the therapy effect. The electrode placing technique is changed one more time by these researchers, when they place anodes and cathodes in an alternate way along the tumor volume, setting them 2 cm away from each other, just as is previously suggested by other authors [Chou et al., 1997].

In June 2005, electrotherapy is used for the first time in Cuba, under the supervision of Dr. Li Jing-Hong from the China-Japan Friendship hospital, located in China, for the treatment of patients with malignant and benign tumors [Jarque et al., 2007]. The study intends to test the electrode insertion procedures and the correct choice in electric charge amount in patients having advanced local tumors who are not recommended for conventional oncology treatment. The study also intends to evaluate the effectiveness and safety of the method. In 1997, Cabrales et al. conducted the first investigations in Cuba on the anti-tumoral effects of electrotherapy, using experimental murine tumors (Ehrlich and fibrosarcoma Sa-37 tumors) in BALB/c, NMRI and C57BL/6 mice. Studies carried out in rats are planned to evaluate the safety and the effects induced by the electrotherapy in tumors and in the body, taking into account the electric charge doses, as well as the number, polarity and orientation of the electrodes, the size and type of the murine tumor and the body characteristics [Cabrales et al., 2001; Ciria et al., 2004; Joa et al., 2010].

In clinical studies, the patient experiences a slight pressure pain or a slight tingling in the treated area during the electrotherapy application. Direct current brings about long lasting pain relief because it inhibits the activity of sensory nerve fibers. In the literature are reported different adverse events (effects), as: fever, wound infections, damages to the blood vessels when the electrodes are inserted close of these [Arsov et al., 2009; Haltiwanger, 2008; Jarque et al., 2007; Li et al., 2006; Salzberg et al., 2008; Vijh, 2006; Vogl et al., 2007; Xin et al., 2004; Yoon et al., 2007].

The underlying mechanisms more widely accepted are the toxic products from of the electrochemical reactions and change of pH. When low voltage (4 to 10 volts) and low amperage (40 to 100 mA) direct currents are administered the tumor area around the anode becomes highly acidic due to the attraction of negatively charged chloride ions and the formation of hydrochloric acid (pH < 3). The tumor areas around the cathode become highly basic (pH > 10) due to the attraction of positively charged sodium ions and the formation of sodium hydroxide. Also, chlorine gas and hydrogen gas emerge from the entry points of the anodes and cathodes, respectively. The pH change depolarizes cancer cell membranes and causes tumors to be gently destroyed [Li et al., 1997; Turjanski et al., 2009; Veiga et al., 2005;

Von Euler et al., 2003]. This suggests that the application of direct current (electric field) causes electrolysis, electrophoresis, electro-osmosis and electroporation in biological tissues, which create micro-environmental chemical changes and micro-electrical field changes [Haltiwanger, 2008; Li et al., 1997]. The chemistry of the microenvironment of healthy cells, injured cells and cancerous cells and the micro-electrical field of these cells are interrelated [Haltiwanger, 2008].

In a previous study [Li et al., 1997] is reported the existence of a group of biochemical alterations around the anode and cathode in tumors under treatment. Around the anode they find a pH of 2, acid hemoglobin, tissue hydration, hydrogen ions that are the result of water electrolysis, and oxygen and chlorine gas emissions. From these emissions they explain the formation of hydrochloric acid and the acid pH. In the cathode, meanwhile, they report a pH of 12, tissue dehydration, hydroxyl ions, which are the result of water electrolysis, and hydrogen gas emissions, from which they explain the formation of sodium hydroxide responsible for the basic pH. Halfway between the electrodes and far from them, no significant differences are observed between the pH and the water concentration in tumors treated with electrotherapy, and those in the untreated tumors. They conclude, then, that the electrochemical effects of this therapy happen around the electrodes.

Other antitumor mechanisms have been reported in the literature, such as: (1) immune system stimulation after treatment (the attraction of white blood cells to the tumor site) [Cabrales et al., 2001; Ciria et al., 2004; Jarque et al., 2007; Serša et al., 1996]; (2) lost of tissue water for electro-osmosis [Li et al., 1997; Vijh, 2004, 2006]; (3) change in the membrane potential of tumor cells, nutrient uptake by tumor cells and reduce deoxyribose nuclei acid production by tumor cells [Chou et al., 1997; Haltiwanger, 2008]; (4) both electrochemical reactions (fundamentally those in which reactive oxygen species are involved) and immune system stimulation induced by cytotoxic action of the direct current, could constitute the most important antitumor mechanisms [Cabrales et al., 2001]; (5) direct current treatment increases the expression of dihydronicotinamide adenine dinucleotide phosphate dehydrogenase (NADPH) oxidase subunits-derived reactive oxygen species which subsequently induces apoptosis of oral mucosa cancer cells [Wartenberg et al., 2008]. These authors also report that an increase of the reactive oxygen species brings about an increase of the expression of heat shock protein (Hsp 70) and Cu/Zn superoxide dismutase (anti-oxidative enzymes) and a decrease of intracellular concentration of reduced glutathione, whereas the expression of catalase remains unchanged.

Some authors evidence apoptosis as tumor dead mechanism after direct electric application [Wartenberg et al., 2008]; however, other report apoptosis and necrosis around anode and necrosis around cathode [Von Euler et al., 2003; Haltiwanger, 2008]. Our experience reveal that the morphologic pattern of necrotic cell mass is the coagulative necrosis 24 hours after direct current application [Cabrales et al., 2001; Ciria et al., 2004; Jarque et al., 2007]. Also, we observe in preclinical and clinical studies vascular congestion, peritumoral neutrophil infiltration, an acute inflammatory response, and a moderate peritumoral monocyte (and macrophages) infiltration, in agreement with other authors [Chou et al., 1997; Li et al., 1997; Serša et al., 1996; Vijh, 2004; Xin et al., 2004]. We are the opinion that apoptosis, necrosis and the electrochemical reactions into tumor (mainly around electrodes) may be explained from reactive oxygen species.

We do not reject the possibility that the electric current density induced into the tumor may affect (directly or indirectly) the cellular membrane, and intracellular and extracellular

spacing that lead to irreversible damages in it. This statement may be corroborated because it has been reported that direct electric current can have significant effects on the symmetry of surface charge, resulting in a change in membrane potential. Electric fields can produce a redistribution of cell surface receptors and influence the flow of specific ions through plasma membrane ion channels [Salzberg et al., 2008; Schaefer et al., 2008]. Any change in the flow of ions through cellular ion channels can have significant effects on cellular metabolism, proliferation rate, cytoplasmic pH, mobility, cell cycle transitions, and apoptosis. Also, research shows that direct electric current application can provide electrons, helping thus to reestablish the biocurrent flows in cancer tissues that are electrically resistant, which brings about the reduction of the resistance, the reestablishing of the transmembrane potential in cancer cells, and the concentration of the sodium, potassium, chlorine and magnesium ions through cell repolarization [Haltiwanger, 2008]. On the other hand, it has been proved that some cell membrane structures can be influenced by the action of the electrical current, the electric field or the accumulated charge. These findings are also found in vitro studies [Haltiwanger, 2008; Joa, 2010; Yen et al., 1999].
Electrotherapy is not implemented in the Clinical Oncology because it is not standardized and its antitumor mechanism is poorly understood. The first reason is explained because the dosage guideline is arbitrary and dose-response relationships are not established. Also, different electrode placements are used and optimal electrode distribution has not been determined [Aguilera et al., 2010; Cabrales et al., 2010; Jiménez et al., 2011; Joa et al., 2010]. The standardization of this therapy from experimental point of view is complex, cumbersome, requires excessive handling of animals, and expensive in resources and time. That is why the mathematical modeling constitutes the core of this chapter.

2.2 Mathematical modeling on electrotherapy: electrode arrays

Computer modeling and simulation keep growing in the more important fields of mathematics and physics applied to biophysics, biology, biochemistry and bioengineering. The reasons for this growing importance are manyfold. Among them, the mathematical modeling has been shown to be a substantial tool for the investigation of complex biophysical, as the cancer. The cancer phenomenon continues to challenge oncologists. The pace of progress has often been slow, in part because of the time required to evaluate new therapies. To reduce the time to approval, new paradigms for assessing therapeutic efficacy are needed. This requires the intellectual energy of scientists working in the field of mathematics and physics, collaborating closely with biologists and clinicians. This essentially means that the heuristic experimental approach, which is the traditional investigative method in the biological sciences, should be complemented by a mathematical modeling approach [Bellomo et al., 2008; Cabrales et al., 2010].
The mathematical modeling has been little exploded in the electrotherapy-cancer topic. Some studies have been focused to propose theoretical models and computer simulations in order to describe the tumor growth kinetics [Cabrales et al., 2008; Cabrales et al., 2010; Miklavčič et al., 1995]. Predicting tumor growth is important in the planning and evaluation of screening programs, clinical trials, and epidemiological studies, as well as in the adequate selection of dose-response relationships regarding the proliferative potential of tumors. Thus, it is apparent that theoretical mathematical models are needed to study cancer [Bellomo et al., 2008; Brú et al., 2003; Jiang, 2009; Mohammadi et al., 2009; Stein et al., 2008].
A modification to the Gompertz equation, named modified Gompertz equation, is made to describe the experimental data of Ehrlich and fibrosarcoma Sa-37 tumor growth kinetics

treated with different direct current intensities [Cabrales et al., 2008]. Fitting the experimental data of CG, TG1, TG2 and TG3 with this modified equation (solid line in Figure 1) suggests that it is feasible to describe the data of untreated and direct current treated tumors. This is also sustained for the small values of the sum of squares of errors (SSE), standard error of the estimate (SE), adjusted coefficient of multiple determination (r_a^2), predicted residual error sum of squares (PRESS), multiple predicted residual sum error of squares (MPRESS) and the errors of each parameter of this equation. This modified Gompertz equation establishes the analytical conditions for which are reached the four tumor responses types after treatment (progressive disease, stable disease, partial response and complete response) and it theoretically corroborates that the electrotherapy antitumor effectiveness increases with the increase of the direct current intensity, as shown in Figure 2 [Cabrales et al., 2008]. Also, this equation theoretically reveals a new antitumor response, named stationary partial response and that these different tumor responses depend on the ratio between the electric current applied to the tumor (i) and that induced in it (i_o), named i/i_o ratio, keeping constant the other parameters of this equation, such as: the initial volume (V_o), the intrinsic growth rate of the tumor (α), the growth deceleration factor (β) related to the antiangiogenic process the growth deceleration factor related to the antiangiogenic process and the duration of the net effect induced in the solid tumor after treatment ($1/\gamma$).

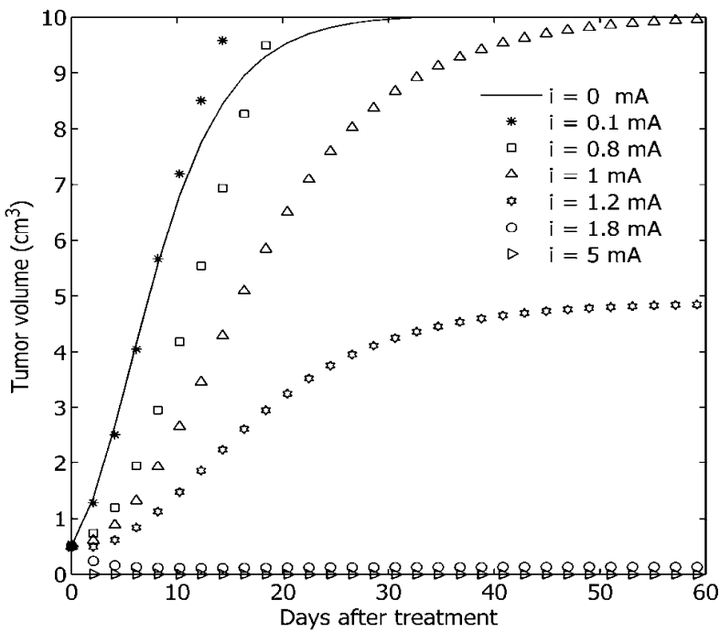

Fig. 2. Simulation of modified Gompertz equation for $\alpha = 0.6$ days^{-1}, $\beta = 0.2$ days^{-1}, $\gamma = 0.016$ days^{-1}, $i_o = 5$ mA, $V_o = 0.5$ cm^3 and different magnitudes of i (mA) [Cabrales et al., 2008].

From modified Gompertz equation, it is easy to verify that the complete and stationary partial responses are reached for $i/i_o > 2$ and $i/i_o = 2$, respectively. This suggests the existence of a threshold value of i/i_o ratio that may be related with the tumor reversibility condition. The tumor complete remission after direct current application suggests that the tumor growth kinetic is completely reversible, as is demonstrated in a previous study. The stationary partial response is characterized first by a significant decrease of the tumor

volume until a certain size, from which it remains constant in the time, fact that may be explained because the organism governs the equilibrium with this small tumor volume that survived to the direct current cytotoxic action. This tumor response type may suggest that the cancer may be a controllable chronic disease [Cabrales et al., 2010].

On the other hand, the mathematical modeling has been used to understand alterations on cellular membrane [Kotnik & Miklavčič, 2006], the role of pH in electrotherapy [Turjanski et al., 2009], the possible physicochemical reactions induced into the tumor during direct current application [Nilsson & Fontes, 2001] and the design of an one-probe two-electrode device in combination with a 3D gel model that contains the cathode and the anode very close to each other (0.1 cm) for studying pH spherical fronts and destroy a cancer cell spherical casket [Olaiz et al., 2010]. Also, the mathematical modeling constitutes a rapid way to propose an optimum electrodes array or close to it, in function of their parameters and those of tumor (localization, size, shape and consistency), using both analytical and numerical solutions. This allows the visualization of the potential, electric field intensity and electric current density distributions generated electrodes arrays in two-dimensional (2D) and three-dimensional (3D) tumors, in order to induce the highest electrotherapy effectiveness (higher tumor destruction with the minimum damage to the organism) [Aguilera et al., 2009; Aguilera et al., 2010; Čorović et al., 2007; Dev et al., 2003; Jiménez et al., 2011; Joa, 2010; Reberšek et al., 2008; Šel et al., 2003]. This later increases our understanding about the current flow inside tumor during direct current application. This is important because monitoring the current flow during aforementioned therapy is a challenging task due to the lack of available noninvasive electrical imaging techniques. We support that the direct current strength and its form of distribution, through electrodes, have potential biomedical applications and a decisive role in the electrotherapy effectiveness [Cabrales et al., 2010; Jiménez et al., 2011].

2D-electrode arrays are useful for planar tumors (basal cell carcinoma of the skin, cutaneous lymphoma, gastric cancer in its form of delinitis, and melanoma in clinical superficial extension) and the potential, electric field strength and electric current density distributions that these induce in the tumor are reported for electrodes circular array [Čorović et al., 2007; Dev et al., 2003; Šel et al., 2003] and electrodes elliptical array [Aguilera et al., 2009; Aguilera et al., 2010]. The explicit dependence of how electric current density distributions depend on the ellipse eccentricity, the ratio between the electric conductivities of the solid tumor (σ_1) and the surrounding healthy tissue (σ_2), named σ_1/σ_2 ratio, and positioning of the electrodes with respect to tumor-surrounding healthy tissue interface is shown in Figures 3 and 4 for an electrodes circular array (eccentricity = 0) and an electrodes elliptical array (eccentricity = 0.85), respectively [Aguilera et al., 2010]. In Figures 3a,d and Figures 4a,d, the electrodes are inserted in the tumor-surrounding healthy tissue interface. Electrodes inserted inside tumor are represented in Figures 3b,e and Figure 4b,e while those inserted in the surrounding healthy tissue are depicted in Figures 3c,f and Figures 4c,f. The influence of σ_1/σ_2 ratio on the electric current density distribution is evidenced for $\sigma_1/\sigma_2 = 1$ (Figures 3a-c and Figures 4a-c) and $\sigma_1/\sigma_2 = 10$ (Figures 3d-f and Figures 4d-f). The other parameters of the electrodes array are constant, such as: electrode radius (a), electrode potential (V_o), electrode polarity (red for the positive electrode, anode, and blue for the negative electrode, cathode), the angular separation between two adjacent-electrodes (θ), major radius (b_1) and minor radius (b_2) of the electrodes array, which are related by means of the eccentricity of it.

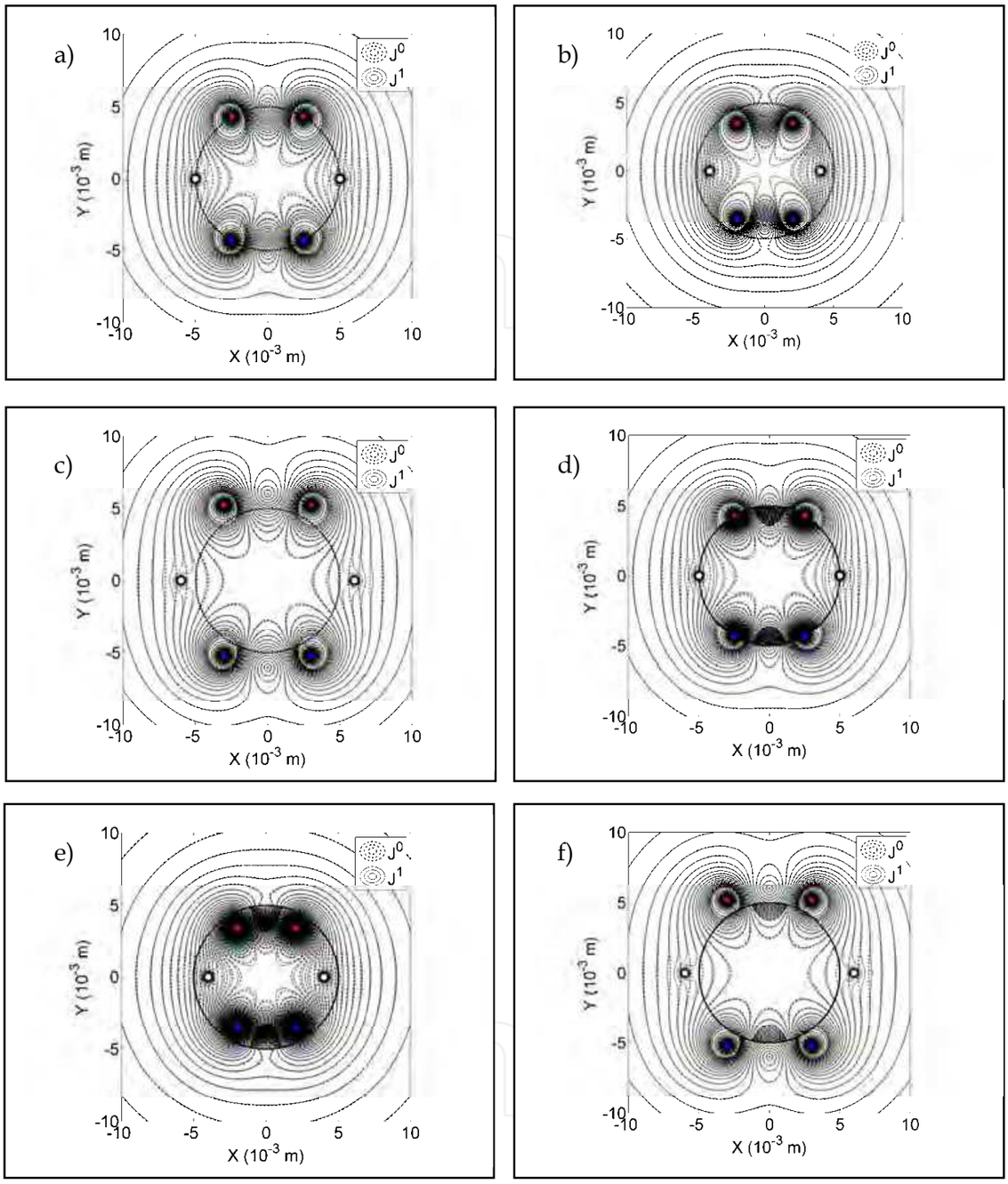

Fig. 3. Distributions of the electric current density, in leading-order, $J^0(x,y)$, and first-order term, $J^1(x,y)$, for an electrodes circular array (eccentricity = 0) for: (a) Configuration 1, $b_1 = b_2 = 0.5$ cm, and $\sigma_1/\sigma_2 = 1$; (b) Configuration 2, $b_1 = b_2 = 0.4$ cm, and $\sigma_1/\sigma_2 = 1$; (c) Configuration 3, $b_1 = b_2 = 0.6$ cm, and $\sigma_1/\sigma_2 = 1$; (d) Configuration 1, $b_1 = b_2 = 0.5$ cm, and $\sigma_1/\sigma_2 = 10$; (e) Configuration 2, $b_1 = b_2 = 0.4$ cm, and $\sigma_1/\sigma_2 = 10$; and (f) Configuration 3, $b_1 = b_2 = 0.6$ cm. These simulations are made for $\theta = 60^o$, $a = 0.0215$ cm, $V_o = +0{,}5$ V for the electrodes 2 and 3, $V_o = -0{,}5$ V for the electrodes 5 and 6, and $V_o = 0$ V for the electrodes 1 and 4. The parameters a, b_1, b_2 (in centimeter) are converted to meter.

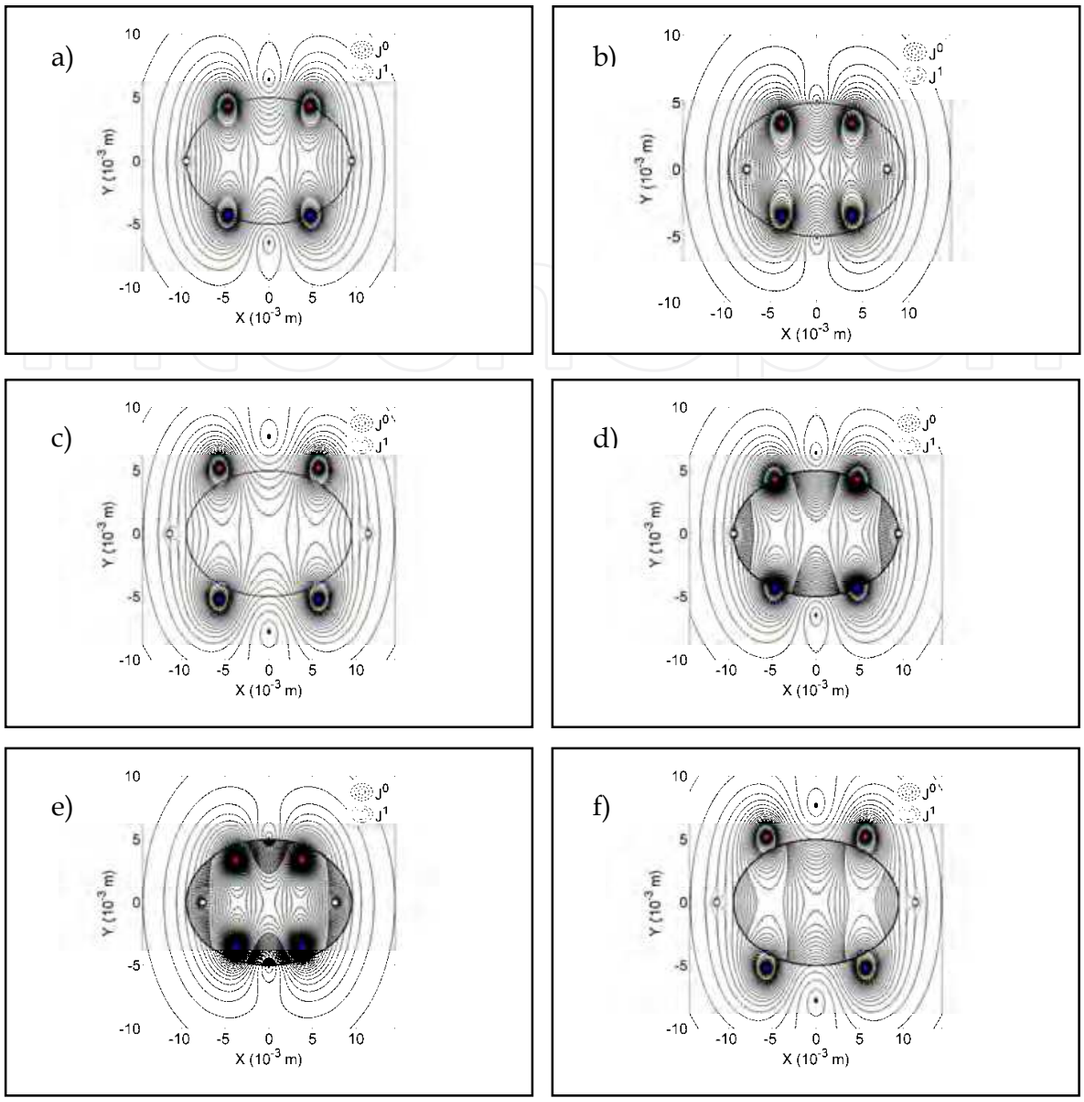

Fig. 4. Distributions of the electric current density, in leading-order, $J^0(x,y)$, and first-order term, $J^1(x,y)$, for an electrodes elliptical array with eccentricity = 0.85 for: (a) Configuration 1, b_1 = 0.9492 cm and b_2 = 0.5 cm, and $\sigma_1/\sigma_2 = 1$; (b) Configuration 2, b_1 = 0.7593 cm and b_2= 0.4 cm, and $\sigma_1/\sigma_2 = 1$; (c) Configuration 3, b_1 = 1.1390 cm and b_2 = 0.6 cm, and $\sigma_1/\sigma_2 = 1$; (d) Configuration 1, b_1= 0.9492 cm and b_2 = 0.5 cm, and $\sigma_1/\sigma_2 = 10$; (e) Configuration 2, b_1= 0.7593 cm and b_2 = 0.4 cm, and $\sigma_1/\sigma_2 = 10$; and (f) Configuration 3, b_1 = 1.1390 cm and b_2 = 0.6 cm, and $\sigma_1/\sigma_2 = 10$. These simulations are made for $\theta = 60^o$, a = 0.0215 cm, V_o = + 0,5 V for the electrodes 2 and 3, V_o = – 0,5 V for the electrodes 5 and 6, and V_o = 0 V for the electrodes 1 and 4. The parameters a, b_1, b_2 (in centimeter) are converted to meter.

In order to get more accurate insight of electric current density (potential and electric field intensity) distribution inside tumor with complex geometries, 3D modeling is studied because, in general, the solid tumors are volumetric. In extending both analytical solution and computational techniques for electric current density from 2D to 3D additional complexities arise, not only because of the 3D geometries but also from the physical nature of the field itself. Also, in this complexity is involved the biological characteristics of the

tissues. 3D solutions are very expensive and should only be undertaken after simpler models have been explored, e.g. the 2D cross-section for the end region for a solid tumor.
There are different analytically ways to calculate the electric current density (electric field) distributions in tissues, as the method based on Green´s theorem (to obtain solutions inside defined volumes in terms of surface values of potential and the normal derivate of potential) and the Clifford analysis (it allows the matching of the electric fields across boundaries separating different conductivity regions with the help of the Clifford product) [Krüger & Menzel, 1996]. We have recently published the analytic solutions that visualize 3D stationary electric current density as a function of the electrode length, tumor size and the conductivities of the tumor (spheroid) and the surrounding healthy tissue (infinite medium) generated by a radial electrode array [Jiménez et al., 2011]. This mathematical formalism is only valid for electrodes inserted along tumor diameters. This particular electrodes configuration may be obtained from a mathematical theorem that allows the calculus of 3D electric current density generated by an array of electrodes with arbitrary shape inserted in an arbitrary region from 3D electric current density induced by a point current source. This guarantees that the electrodes may be inserted in any place of the tumor.

2.2.1 3D stationary electric current density generated by a wire from a point current source

There is a three-dimensional, conductive, heterogeneous region consisting of two linear, homogeneous, isotropic media separated by an interface Σ. Medium 1 of constant mean conductivity σ_1 (in S/m) and Medium 2 of constant mean conductivity σ_2 (in S/m) are considered as homogeneous conducting media, as shown in Figure. 5a for the point current source and in Figures. 5b,c for a wire of length L, which are inserted inside the Medium 1.

2.2.2 Point current source

We consider that current is continuous and the magnetic field associated to it may be neglected (≤ 0.02 Gauss) then the calculus of the potential φ in the point $\vec{r}$ generated by a point current source with current intensity I located inside tumor in the point $\vec{r}_0$ (Figure 5a) yield to the following boundary-value problem, named Problem 0

$$\begin{cases} \nabla^2 \varphi_1 = -\dfrac{I}{\sigma_1}\delta\left(\vec{r}-\vec{r}_0\right) \\ \nabla^2 \varphi_2 = 0 \end{cases} \tag{1}$$

$$\begin{cases} \varphi_1\big|_\Sigma = \varphi_2\big|_\Sigma \\ \sigma_1 \dfrac{\partial \varphi_1}{\partial \hat{n}}\bigg|_\Sigma = \sigma_2 \dfrac{\partial \varphi_2}{\partial \hat{n}}\bigg|_\Sigma \\ \lim\limits_{r\to\infty} |\varphi_2| < \infty \end{cases} \tag{2}$$

where $\varphi_i\big|_\Sigma$ and $\partial\varphi_i/\partial\hat{n}\big|_\Sigma$ (i = 1, 2) are the potential and its normal derivative in the surface Σ that separate both mediums.

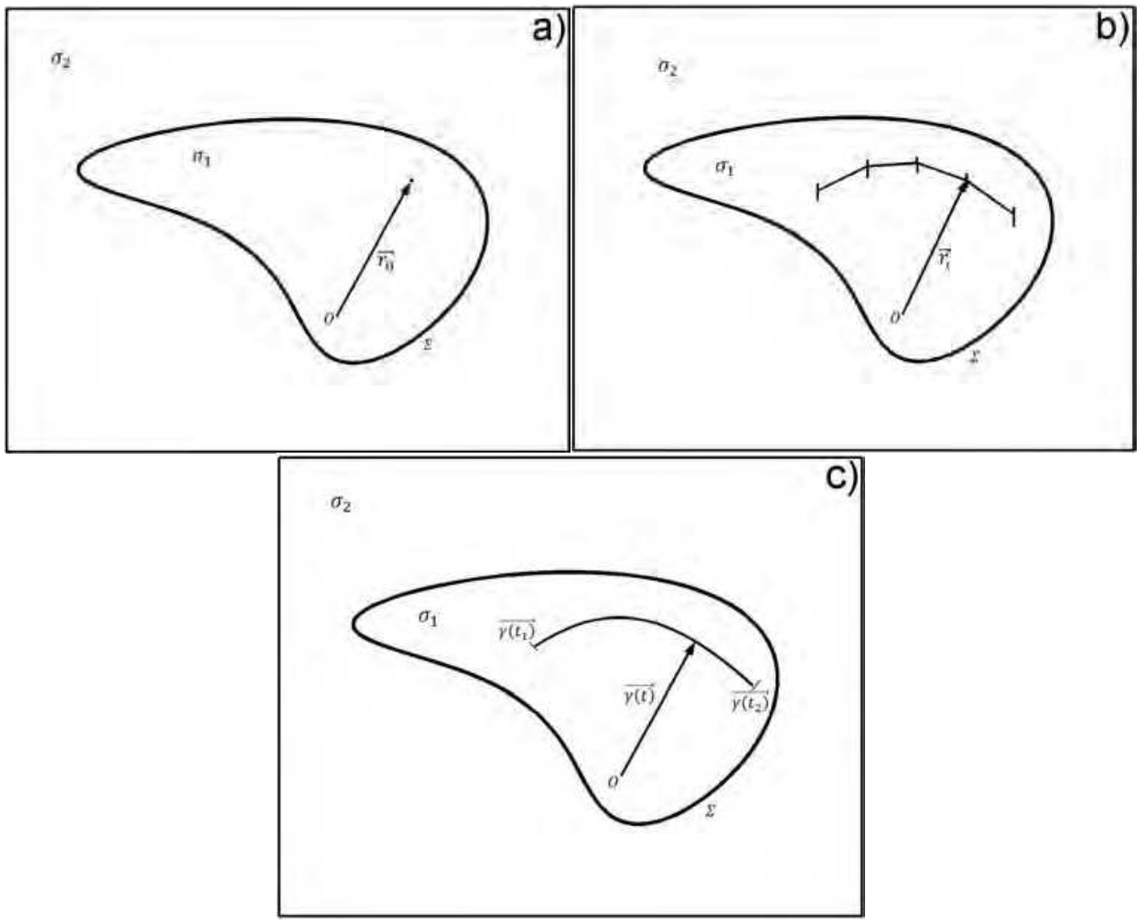

Fig. 5. Schematic representation of (a) a point electrode, (b) a wire subdivided in *N* small pieces of longitude δl and (c) a whole wire with ends $\vec{\gamma}(t_1)$ and $\vec{\gamma}(t_2)$ located in the Medium 1 of conductivity σ_1 surrounded of a Medium 2 of conductivity σ_2. The axis *y* is perpendicular to the paper (toward us out of the page).

2.2.3 Electrode in form of wire of length finite

Instead of a point current source we now assume the case of a wire of length L (Figure 5c) analytically represented for the following parametric differentiable form of the curve $\vec{\gamma}(t)$ of parameter t

$$\vec{\gamma}(t) = \big(x(t), y(t), z(t)\big), \quad t \in [t_1, t_2] \tag{3}$$

The wire is subdivided in N small pieces of longitude δl (Figure 5b), so that the first equation of the system (1) can re-write as

$$\nabla^2 \psi_1 \approx -\frac{I}{\sigma_1 L} \sum_{i=1}^{N} \delta\big(\vec{r} - \vec{\gamma}(t_i)\big) \delta l_i \tag{4}$$

with

$$L = \int_{t_1}^{t_2} \left\| \frac{d\vec{\gamma}}{dt} \right\| dt \tag{4a}$$

$$\left\| \frac{d\vec{\gamma}}{dt} \right\| = \sqrt{\left(\frac{dx}{dt}\right)^2 + \left(\frac{dy}{dt}\right)^2 + \left(\frac{dz}{dt}\right)^2} \tag{4b}$$

and

$$\delta l_i = \left\| \frac{d\vec{\gamma}}{dt} \right\|_{t=t_i} \Delta t \tag{4c}$$

where ψ_1 is the potential generated in the tumor by the wire electrode. $\|d\vec{\gamma}/dt\|$ is the modulus of the tangent to $\vec{\gamma}(t)$ in Cartesian coordinates, $\Delta t = (t_2\text{-}t_1)/N$ is the variation of t. When $\Delta t \to 0$ (in the limit $N \to \infty$) results the following boundary-value problem (named Problem 1)

$$\begin{cases} \nabla^2 \psi_1 = -\dfrac{I}{\sigma_1 L} \displaystyle\int_{t_1}^{t_2} \delta\left(\vec{r} - \vec{\gamma}(t_i)\right) \left\| \frac{d\vec{\gamma}}{dt} \right\| dt \\ \nabla^2 \psi_2 = 0 \end{cases} \tag{5}$$

$$\begin{cases} \psi_1\big|_\Sigma = \psi_2\big|_\Sigma \\ \sigma_1 \dfrac{\partial \psi_1}{\partial \hat{n}}\bigg|_\Sigma = \sigma_2 \dfrac{\partial \psi_2}{\partial \hat{n}}\bigg|_\Sigma \\ \lim\limits_{r \to \infty} |\psi_2| < \infty \end{cases} \tag{6}$$

where ψ_1 and $\partial\psi_1/\partial\hat{n}$ are the potential and normal derivative of the potential in Medium 1, respectively. ψ_2 and $\partial\psi_2/\partial\hat{n}$ are these magnitudes but in Medium 2. $\hat{n}$ is the unit normal vector to the surface Σ (directed from Medium 1 to Medium 2). δ is the Dirac delta. $\vec{r}$ is the position of the spherical coordinate.

The solution of the Problem 1 may be expressed in a very simple way starting from the solution of the Problem 0 by means the following theorem

2.2.4 Theorem

Let be $\varphi_i(\vec{r}, \vec{r}_0)$, i = 1,2, the solution of the Problem 0. Then, the solution of the Problem 1 is

$$\psi_i(\vec{r}) = \frac{1}{L} \int_{t_1}^{t_2} \varphi_i\left(\vec{r}, \vec{\gamma}(t)\right) \left\| \frac{d\vec{\gamma}}{dt} \right\| dt \tag{7}$$

The demonstration is immediate simply if we substitute (7) in (5) and (6). Substituting (7) in (5) results

$$\nabla^2 \psi_i(\vec{r}) = \nabla^2 \frac{1}{L} \int_{t_1}^{t_2} \varphi_i\left(\vec{r}, \vec{\gamma}(t)\right) \left\| \frac{d\vec{\gamma}}{dt} \right\| dt = \frac{1}{L} \int_{t_1}^{t_2} \nabla^2 \varphi_i\left(\vec{r}, \vec{\gamma}(t)\right) \left\| \frac{d\vec{\gamma}}{dt} \right\| dt \tag{8}$$

Making $\vec{r}_0 = \vec{\gamma}(t)$ in (1) and substituting in (8) result (5). Also, it can be demonstrated that (7) satisfies the boundary conditions (6).

To illustrate the theorem above mentioned, we use the particular case of a radial electrode array proposed in a previous study [Jiménez et al., 2011]. A three-dimensional, conductive, heterogeneous region consists of two linear, homogeneous, isotropic media (tumor and the surrounding healthy tissue) separated by an interface Σ. Solid tumor (Medium 1) is considered as a homogeneous conducting sphere of radius R (in m) and constant mean conductivity σ_1 (in S/m). The surrounding healthy tissue (Medium 2) is supposed to be a homogeneous infinite medium of constant mean conductivity σ_2 (in S/m), as shown in Figure 6a.

Point electrode and wire are inserted in plane y = 0 m along tumor diameters and in (r_0,0,0), using the system of spherical coordinates with the origin in the center of the sphere, as shown in Figures 6b (one current source) and 6c (two current sources), respectively. In the particular case that both electrode types are located in the axis z (the radial coordinate in spherical coincides with axis z of the Cartesian coordinate or (0,0,r_0)).

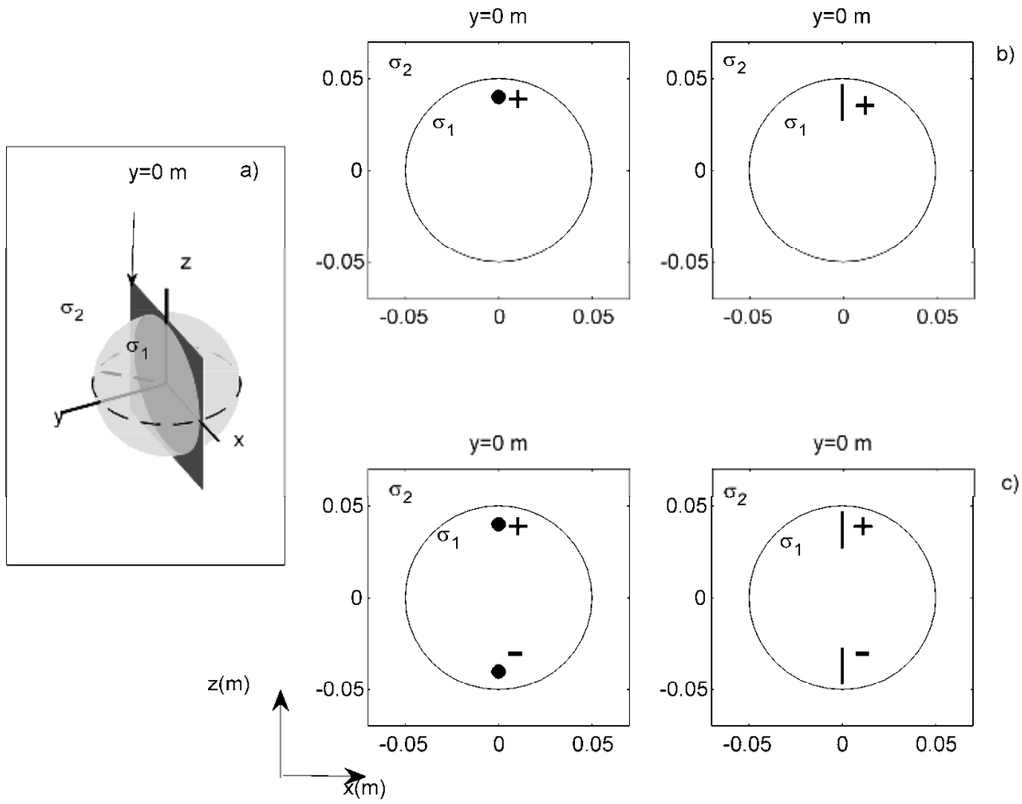

Fig. 6. (a) Spherical tumor of conductivity σ_1 (in S/m) and radius R (in m) surrounded by its healthy tissue of conductivity σ_2 (in S/m) and separated by the interface Σ. (b) A point electrode (positive) and an electrode with form of wire (positive) are inserted along tumor diameter (plane y = 0 cm). (c) Two point electrodes 1 (one positive and another negative) and two electrodes with form of wire (one positive and another negative) are inserted along tumor diameter (plane y = 0 cm).

As the point electrode is located in the tumor along the axis z (left picture in Figure 6a), the solution of the Problem 0 is given by

$$\varphi_1 = \frac{I}{4\pi\sigma_1}\frac{1}{\sqrt{r_0^2 + r^2 - 2rr_0\cos\theta}} + \sum_{n=0}^{\infty} A_n r^n P_n(\cos\theta) \tag{9}$$

$$\varphi_2 = \sum_{n=0}^{\infty} B_n r^{-(n+1)} P_n(\cos\theta) \tag{10}$$

The coefficients A_n and B_n are obtained of the boundary conditions (2), resulting

$$\varphi_1 = \frac{I}{4\pi\sigma_1}\frac{1}{\sqrt{r_0^2 + r^2 - 2rr_0\cos\theta}} + \frac{I}{4\pi}\left(\frac{\sigma_1 - \sigma_2}{\sigma_1}\right)\sum_{n=0}^{\infty}\frac{(n+1)r_0^n r^n P_n(\cos\theta)}{R^{2n+1}\left[n\sigma_1 + (n+1)\sigma_2\right]} \tag{11}$$

$$\varphi_2 = \frac{I}{4\pi}\sum_{n=0}^{\infty}\frac{(2n+1)r_0^n P_n(\cos\theta)}{r^{(n+1)}\left[n\sigma_1 + (n+1)\sigma_2\right]} \tag{12}$$

Starting from (11) and (12), corresponding to a point electrode, we can pass to the solution of the potential generated by a wire with ends in a and b inserted in the tumor along the axis z (right picture in Figure 6b). In this particular case, the parametric equations of the wire are

$$\begin{cases} x = 0 \\ y = 0 \\ z = t \end{cases} \tag{13}$$

In this case, L = b-a and $\left\|d\vec{\gamma}/dt\right\| = 1$. Substituting (13), L and $\left\|d\vec{\gamma}/dt\right\|$ in (7), we obtain the solutions for the wire, given by

$$\psi_1 = \frac{1}{(b-a)}\int_{t_t}^{t_2}\left[\frac{I}{4\pi\sigma_1}\frac{1}{\sqrt{t^2 + r^2 - 2rt\cos\theta}} + \frac{I}{4\pi}\left(\frac{\sigma_1 - \sigma_2}{\sigma_1}\right)\sum_{n=0}^{\infty}\frac{(n+1)t^n r^n P_n(\cos\theta)}{R^{2n+1}\left[n\sigma_1 + (n+1)\sigma_2\right]}\right]dt \tag{14}$$

$$\psi_2 = \frac{1}{(b-a)}\int_{t_1}^{t_2}\frac{I}{4\pi}\sum_{n=0}^{\infty}\frac{(2n+1)t^n P_n(\cos\theta)}{r^{(n+1)}\left[n\sigma_1 + (n+1)\sigma_2\right]}dt \tag{15}$$

Integrating (14) and (15) from t = a to t = b, we have

$$\begin{aligned}\psi_1 = \frac{I}{4\pi(b-a)}\Bigg\{&\frac{1}{\sigma_1}\ln\left[\frac{\sqrt{b^2 + r^2 - 2br\cos\theta} + b - r\cos\theta}{\sqrt{a^2 + r^2 - 2ar\cos\theta} + a - r\cos\theta}\right] \\ &+\left(\frac{\sigma_1 - \sigma_2}{\sigma_1}\right)\sum_{n=0}^{\infty}\frac{\left(b^{n+1} - a^{n+1}\right)r^n P_n(\cos\theta)}{R^{2n+1}\left[n\sigma_1 + (n+1)\sigma_2\right]}\Bigg\}\end{aligned} \tag{16}$$

$$\psi_2 = \frac{I}{4\pi(b-a)}\sum_{n=0}^{\infty}\frac{(2n+1)\left(b^{n+1}-a^{n+1}\right)P_n(\cos\theta)}{(n+1)r^{(n+1)}\left[n\sigma_1+(n+1)\sigma_2\right]} \tag{17}$$

The superposition principle is used when two (Figs. 6c,d) or more current sources are inserted in the tumor. From (11), (12), (16) and (17) may be determined the electric field intensity ($\vec{E} = -\nabla\varphi$) and the electric current density ($\vec{J} = -\sigma\nabla\varphi$) inside and outside the tumor for a point current source ($\left|\vec{J}_{1p}\right|$ and $\left|\vec{J}_{2p}\right|$ are the current densities inside and outside, respectively) [Jiménez et al., 2011; Joa, 2010] and a wire of length L ($\left|\vec{J}_{1w}\right|$) and ($\left|\vec{J}_{2w}\right|$ are the current densities inside and outside, respectively), which are given by

$$\left|\vec{J}_{ip}\right| = \sigma\sqrt{\left(\frac{\partial\varphi_i}{\partial r}\right)^2+\left(\frac{\partial\varphi_i}{r\partial\theta}\right)^2} \quad \text{(i = 1,2)} \tag{18}$$

with

$$\frac{\partial\varphi_1}{\partial r} = \frac{I}{4\pi}\left\{\frac{1}{\sigma_1}\frac{r-r_0\cos\theta}{(r_0^2+r^2-2rr_0\cos\theta)^{3/2}}+\left(\frac{\sigma_1-\sigma_2}{\sigma_1}\right)\sum_{n=0}^{\infty}\frac{(n+1)r_0^n r^{n-1}P_n(\cos\theta)}{R^{2n+1}\left[n\sigma_1+(n+1)\sigma_2\right]}\right\} \tag{19}$$

$$\frac{\partial\varphi_1}{r\partial\theta} = \frac{I}{4\pi}\left\{-\frac{1}{\sigma_1}\frac{r_0 sen\theta}{(r_0^2+r^2-2rr_0\cos\theta)^{3/2}}+\left(\frac{\sigma_1-\sigma_2}{\sigma_1}\right)\sum_{n=0}^{\infty}\frac{(n+1)r_0^n r^{n-1}T_n(\cos\theta)}{R^{2n+1}\left[n\sigma_1+(n+1)\sigma_2\right]}\right\} \tag{20}$$

$$\frac{\partial\varphi_2}{\partial r} = -\frac{I}{4\pi}\sum_{n=0}^{\infty}\frac{(2n+1){r_0}^n P_n(\cos\theta)}{r^{(n+2)}\left[n\sigma_1+(n+1)\sigma_2\right]} \tag{21}$$

$$\frac{\partial\varphi_2}{r\partial\theta} = \frac{I}{4\pi}\sum_{n=0}^{\infty}\frac{(2n+1){r_0}^n T_n(\cos\theta)}{r^{(n+2)}\left[n\sigma_1+(n+1)\sigma_2\right]} \tag{22}$$

$$T_n = -sen\theta\left[\frac{n\cos\theta\, P_n(\cos\theta)-n\, P_{n-1}(\cos\theta)}{\cos^2\theta-1}\right] \tag{23}$$

where $\partial\varphi_i/\partial r$ and $\partial\varphi_i/r\partial\theta$ are the radial and angular components of electric field vector for inside (i = 1) and outside (i = 2) the tumor, respectively

$$\left|\vec{J}_{iw}\right| = \sigma\sqrt{\left(\frac{\partial\psi_i}{\partial r}\right)^2+\left(\frac{\partial\psi_i}{r\partial\theta}\right)^2} \quad \text{(i = 1,2)} \tag{24}$$

with

$$\frac{\partial\psi_1}{\partial r} = \frac{I}{4\pi(b-a)}\left\{\frac{A(a,b,r,\theta)}{\sigma_1}+\left(\frac{\sigma_1-\sigma_2}{\sigma_1}\right)\sum_{n=0}^{\infty}\frac{n\left(b^{n+1}-a^{n+1}\right)r^{n-1}P_n(\cos\theta)}{R^{2n+1}\left[n\sigma_1+(n+1)\sigma_2\right]}\right\} \tag{25}$$

$$\frac{1}{r}\frac{\partial \psi_1}{\partial \theta} = \frac{I}{4\pi(b-a)}\left\{\frac{B(a,b,r,\theta)}{\sigma_1} + \left(\frac{\sigma_1-\sigma_2}{\sigma_1}\right)\sum_{n=0}^{\infty}\frac{\left(b^{n+1}-a^{n-1}\right)r^{n-1}T_n}{R^{2n+1}\left[n\sigma_1+(n+1)\sigma_2\right]}\right\} \tag{26}$$

$$\frac{\partial \psi_2}{\partial r} = -\frac{I}{4\pi(b-a)}\sum_{n=0}^{\infty}\frac{(2n+1)\left(b^{n+1}-a^{n+1}\right)P_n(\cos\theta)}{r^{(n+2)}\left[n\sigma_1+(n+1)\sigma_2\right]} \tag{27}$$

$$\frac{1}{r}\frac{\partial \psi_2}{\partial \theta} = \frac{I}{4\pi(b-a)}\sum_{n=0}^{\infty}\frac{(2n+1)\left(b^{n+1}-a^{n+1}\right)T_n}{(n+1)r^{(n+2)}\left[n\sigma_1+(n+1)\sigma_2\right]} \tag{28}$$

where

$$A(a,b,r,\theta) = \frac{\dfrac{r-b\cos\theta}{\sqrt{b^2+r^2-2br\cos\theta}} - \cos\theta}{\sqrt{b^2+r^2-2br\cos\theta}+b-r\cos\theta} - \frac{\dfrac{r-a\cos\theta}{\sqrt{a^2+r^2-2ar\cos\theta}} - \cos\theta}{\sqrt{a^2+r^2-2ar\cos\theta}+a-r\cos\theta} \tag{29}$$

$$B(a,b,r,\theta) = \frac{\dfrac{bsen\theta}{\sqrt{b^2+r^2-2br\cos\theta}} + sen\theta}{\sqrt{b^2+r^2-2br\cos\theta}+b-r\cos\theta} - \frac{\dfrac{asen\theta}{\sqrt{a^2+r^2-2ar\cos\theta}} + sen\theta}{\sqrt{a^2+r^2-2ar\cos\theta}+a-r\cos\theta} \tag{30}$$

T_n in (26) and (28) is given by (23). $\partial\psi_i/\partial r$ and $\partial\psi_i/r\partial\theta$ are the radial and angular components of electric field vector for inside (i = 1) and outside (i = 2) the tumor, respectively.

Figure 7 shows the isolines of $\left|\vec{J}_{1p}\right|$ and $\left|\vec{J}_{2p}\right|$ (Fig. 7a), and $\left|\vec{J}_{1w}\right|$ and $\left|\vec{J}_{2w}\right|$ (Figure 7b) in different planes of the sphere(y = 0.1, 2 and 4 cm) parallel to the plane that contains the electrodes (y = 0 cm) for a point current source and a wire, respectively. The point current source is located in r_0 = 4 cm (Figure 5a) whereas the wire with ends in a = 1 cm and b = 4 cm (L = 3 cm), as shown in Figure 5b. In both figures, we fix σ_1 = 0.4 S/m, σ_2 = 0.2 S/m, I = 5 mA and R = 5 cm. Figures 7a and 7b reveal that there are differences between the distributions of $\left|\vec{J}_{1p}\right|$ and $\left|\vec{J}_{1w}\right|$; however, non significant differences are observed between these distributions of $\left|\vec{J}_{1w}\right|$ and $\left|\vec{J}_{2w}\right|$ for different values of L. These differences are shown in Table 1 and are quantified by means of the maximum difference (D_{max}, in A/m^2) and the Root Means Square Error (RMSE, in A/m^2), given by

$$D_{\max} = \max\left\|\left|\vec{J}_{wi}\right| - \left|\vec{J}_{pi}\right|\right\|, \quad \text{(i = 1, 2)} \tag{31}$$

$$RMSE = \sqrt{\sum_{i=1}^{M}\frac{\left(\left|\vec{J}_{wi}\right| - \left|\vec{J}_{pi}\right|\right)^2}{M}} \quad \text{(i = 1, 2)} \tag{32}$$

where J_{pi} are the *i-th* calculated values of $J_p(x,y)$ and J_{wi} are the *i-th* calculated values of $J_w(x,y)$ for different values of L (0.5, 1, 1.5, 2, 2.5 and 3 cm). M is the number of points where $\left|\vec{J}_{1p}\right|$ ($\left|\vec{J}_{1w}\right|$) and $\left|\vec{J}_{2p}\right|$ ($\left|\vec{J}_{2w}\right|$) are calculated.

$\Im_1$ ($\Im_1 = \sqrt{\sum_{k=1}^{m_1}\left|\vec{J}_{1k}\right|^2}$: sum of the local current density over all points in the tumor) and $\Im_2$ ($\Im_2 = \sqrt{\sum_{k=1}^{m_2}\left|\vec{J}_{2k}\right|^2}$: sum of the local current density over all points in a region of the surrounding healthy tissue) are used in the figures to compare the overall effect of changing of L on $\left|\vec{J}_{1p}\right|$ ($\left|\vec{J}_{1w}\right|$) and $\left|\vec{J}_{2p}\right|$ ($\left|\vec{J}_{2w}\right|$). $\Im_1$ and $\Im_2$ are evaluated in a set of discrete points m_1 and m_2, respectively, for both point current source and wire. $\Im_1$ is calculated in all tumor volume (m_1 = 84 050 points) except in the points where the electrodes are inserted and in their vicinities. $\Im_2$ is also calculated in the surrounding healthy tissue (m_2 = 35 301 points) comprehended in a spherical cap (between R (5 cm) and R + 2 (7 cm)). Table 2 reveals that $\Im_1$ and $\Im_2$ for the point current source are higher than those for the wire for all value of L. For the wire, it is observed that an increase of *L* results in a decrease of $\Im_2$ whereas inside to the tumor $\Im_1$ first decreases (up to *L* = 2 cm) and then increases. The behavior of $\Im_1$ with *L* is given in [Jiménez et al., 2011].

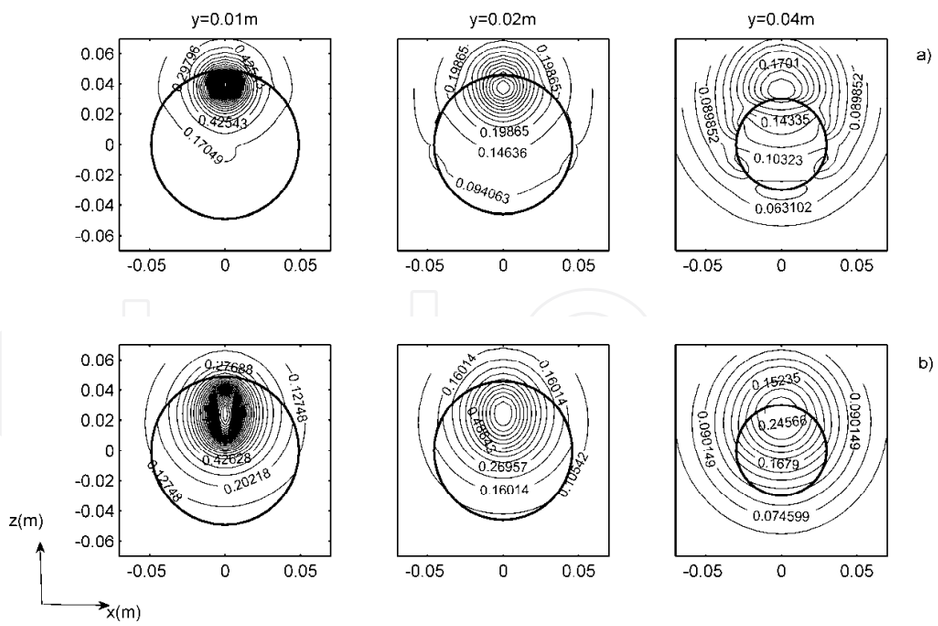

Fig. 7. Projections of $\left|\vec{J}_{1p}\right|$ (in A/m²) and $\left|\vec{J}_{2p}\right|$ (in A/m²) on planes *y* = 0.1, 2 and 4 cm for (a) one point electrode and (b) one electrode with form of wire ($\left|\vec{J}_{1w}\right|$, in A/m², and $\left|\vec{J}_{2w}\right|$, in A/m²). In each figure, the electrode polarity is positive (see Figure 6b).

Type of current source		Electric current density in the tumor (A/m²)		Electric current density in the surrounding healthy tissue (A/m²)	
		D_{max}	RMSE	D_{max}	RMSE
Point		0	0	0	0
Wire	L = 0.5 cm	39744.718	3.0283	0.537	0.0003
	L = 1 cm	39763.700	3.0296	0.877	0.0006
	L = 1.5 cm	39771.290	3.0302	1.103	0.0007
	L = 2 cm	39775.324	3.0305	1.262	0.0008
	L = 2.5 cm	39777.820	3.0307	1.379	0.0009
	L = 3 cm	39779.514	3.0309	1.468	0.0010

Table 1. D_{max} and RMSE of $\left|\vec{J}_{1w}\right|$ (in A/m²) and $\left|\vec{J}_{2w}\right|$ (in A/m²) for a wire of length L respect to $\left|\vec{J}_{1p}\right|$ (in A/m²) and $\left|\vec{J}_{2p}\right|$ (in A/m²) generated by a point current source. L varies from 0.5 to 3 cm.

Type of current source		$\Im_1$ (A/m²)	$\Im_2$ (A/m²)
Point		254800	63.080
Wire	L = 0.5 cm	1201.378	52.630
	L = 1 cm	1065.803	45.676
	L = 1.5 cm	1003.083	40.762
	L = 2 cm	996.252	37.128
	L = 2.5 cm	1045.207	34.344
	L = 3 cm	1182.477	32.155

Table 2. $\Im_1$ (norm of $\left|\vec{J}_{1p}\right|$ for a point electrode or $\left|\vec{J}_{1w}\right|$ for a wire) and $\Im_2$ (norm of $\left|\vec{J}_{2p}\right|$ for a point electrode or $\left|\vec{J}_{2w}\right|$ for a wire). The wire length is L (between 0.005 to 0.030 m). $\Im_1$ and $\Im_2$ are given in A/m².

The distributions of $\left|\vec{J}_{1p}\right|$, $\left|\vec{J}_{2p}\right|$, $\left|\vec{J}_{1w}\right|$ and $\left|\vec{J}_{2w}\right|$ for two point electrodes and two wires are shown in Figures 8a and 8b, respectively. The differences between these distributions are also quantified by means of D_{max} and RMSE (Table 3) and the values of $\Im_1$ and $\Im_2$ evaluated in the same discrete points m_1 and m_2 are given in Table 4. A comparison of Figures 7 and 8 reveals that an increase of the number of current sources (point or wire) results in a higher distribution of the electric current density lines in the tumor, being more evident for the electrodes in form of wire.

For the calculations of $\left|\vec{J}_{1p}\right|$, $\left|\vec{J}_{2p}\right|$, $\left|\vec{J}_{1w}\right|$, $\left|\vec{J}_{2w}\right|$, RMSE, D_{max}, $\Im_1$ and $\Im_2$, the unities of y, a, b, L and R, given in cm, are converted to meter.

The 3D-analytical expressions shown in this chapter allow the visualization of the potential, electric field strength and electric current density distributions generated for point current

Type of current source		Electric current density in the tumor (A/m²)		Electric current density in the surrounding healthy tissue (A/m²)	
		D_{max}	RMSE	D_{max}	RMSE
Point		0	0	0	0
Wire	L = 0.5 cm	39744.681	4.2824	0.564	0.0005
	L = 1 cm	39763.672	4.2845	0.918	0.0008
	L = 1.5 cm	39771.267	4.2854	1.152	0.0011
	L = 2 cm	39775.306	4.2858	1.317	0.0012
	L = 2.5 cm	39777.807	4.2861	1.440	0.0014
	L = 3 cm	39779.507	4.2863	1.537	0.0015

Table 3. D_{max} and RMSE of $\left|\vec{J}_{1w}\right|$ (in A/m²) and $\left|\vec{J}_{2w}\right|$ (in A/m²) for an array of two equal wires with different lengths L (between 0.5 to 3 cm) respect to those generated by an array of two point electrodes ($\left|\vec{J}_{1p}\right|$, in A/m², and $\left|\vec{J}_{2p}\right|$, in A/m²).

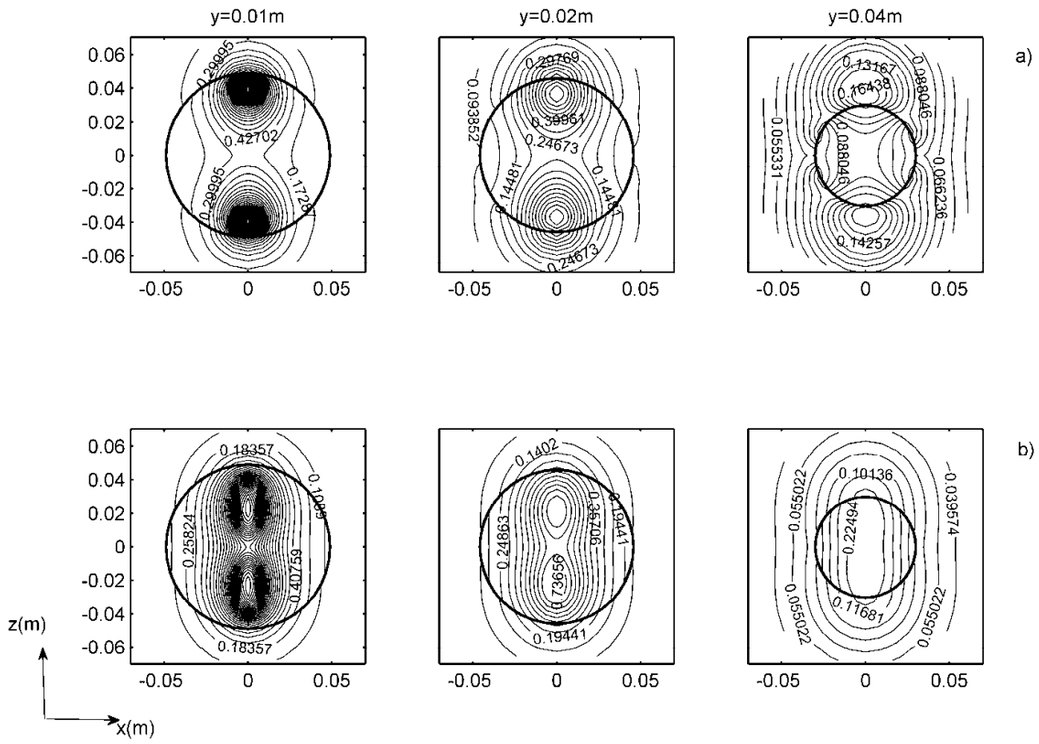

Fig. 8. Projections of $\left|\vec{J}_{1p}\right|$ (in A/m²) and $\left|\vec{J}_{2p}\right|$ (in A/m²) on planes y = 0.1, 2 and 4 cm for (a) two point electrodes and (b) two electrodes with forms of wire ($\left|\vec{J}_{1w}\right|$, in A/m², and $\left|\vec{J}_{2w}\right|$, in A/m²). In each figure, one electrode is positive and another is negative (Figure 6c).

Type of current source		$\Im_1$ (A/m^2)	$\Im_2$ (A/m^2)
Point		360340	82.912
Wire	L = 0.5 cm	1702.887	66.861
	L = 1 cm	1512.207	55.909
	L = 1.5 cm	1424.731	47.906
	L = 2 cm	1416.607	41.710
	L = 2.5 cm	1488.047	36.679
	L = 3 cm	1685.969	32.432

Table 4. $\Im_1$ (norm of $\left|\vec{J}_{1p}\right|$ for two point electrodes or $\left|\vec{J}_{1w}\right|$ for two wires) and $\Im_2$ (norm of $\left|\vec{J}_{2p}\right|$ for two point electrodes or $\left|\vec{J}_{2w}\right|$ for two wires). The wires are equals and have different lengths L (from 0.5 to 3 cm). $\Im_1$ and $\Im_2$ are given in A/m^2.

sources and radial arrays of electrodes with finite length. The results of the simulations reveal as these distributions in the tumor and its surrounding healthy tissue change in function of the tumor size, the positioning, number and polarity of the electrodes, and the difference of electrical conductivity between both tissues for, in agreement with previous theoretical studies [Aguilera et al., 2009; Aguilera et al. 2010; Čorović et al., 2007; Jiménez et al., 2011; Joa, 2010; Reberšek et al., 2008; Šel et al., 2003] and experimental reports [Chou et al., 1997; Ren et al., 2001; Serša et al., 1997; Turler et al., 2000; Xin et al., 1994; Yoon et al., 2007].

3D-analytical expressions for the potential, electric field intensity and electric current density generated by wires completely inserted in the tumor along their diameters (plane y = 0 cm) are directly obtained from the application of this mathematical theorem and the parametric form of the curve given in equation (3). This justify that equations (16) and (17) are correct from the substitution of I for $\delta I = I/(b-a)dr_0$ in equations (14) and (15) and then integrating these expressions from $r_0 = a$ to $r_0 = b$, as is suggested in a previous study [Jiménez et al., 2011].

Non-uniform current density distributions are shown in a tumor (homogeneous conductor spheroid), as shown in Figures 7 (point electrodes) and 8 (electrodes with forms of wire). Normally, needles electrodes have highly non-homogeneous fields around their tips due to the sharp geometry. There are marked differences between the electric current density (potential and electric field) patterns generated by a point electrodes array and arrays of electrodes with length L, as is expected. Electric current density near the electrodes is also imaged for both point and wire arrays. Although the electric current density is maximum near electrodes, the magnitude of it fall even more rapidly towards the tumor edges in the perpendicular direction to the plane in which are the electrodes. Tumor regions unaffected by this electric current density re-grow after treatment. The singularities observed where the electrodes contact the tumor (large electric fields at the edges) can be avoided by grading the electric field near such edges. High current densities in the vicinity of the electrodes may result in tissue damage (example, coagulative necrosis), in agreement with our observations in mice [Cabrales et al., 2001; Ciria et al., 2004] and patients [Jarque et al., 2007]. Moreover, measurement of current density distribution near the current injecting electrodes provides information on the behavior of the electrode-tissue interface. Up to now, it has not discussed as depends on the electrotherapy antitumor effectiveness in function of the homogeneity

degree of the electric current density (electric field) induced in the tumor, essential aspect in the design of electrodes array and treatment planning.

The insertion of the electrodes along tumor diameters is a particular electrodes array that we have used in some patients whose tumor thickness (depth) is smaller respect to their other two dimensions (skin, breast and vulva cancers) when the conventional therapies fail or cannot be applied, as shown in Figure 9. A direct current of 10 mA for 60 min is delivered to this patient with vulva cancer through 19 electrodes inserted with alternate polarities and it is generated by ZAY-6B electric device (manufactured in Chinese). Cannulae with trocar are inserted into the tumor mass under local anesthesia and the number of these depends on the tumor size (20 cm in diameter). The cannulae are fixed with a distance (gap) between them of 1 cm and disposed along a semi-circumference because for this zone pass important blood vessels. This distance should not be further than 1.5 cm apart because the tumor killing area around the needle is about 2 cm in diameter. Then the trocar are withdrawn and electrodes are inserted into the tumor through the cannulae to ensure that the electric field will cover all the tumor mass when the direct current passes through electrodes. After insertion of the electrodes, the cannulae are withdrawn to the edge of normal tissue by palpation with hand. These cannulae in the edge are insulation tubes to protect the normal tissue from the injury due to electrolysis. This procedure guarantees that the electrodes are completely inserted into the solid tumor to maximize tumor destruction with the minimum damage in the organism. The electrodes are then connected to the cathode or anode of the ZAY-6B device to supply the direct current that pass through the solid tumor. This procedure guarantees that the electrodes are completely inserted into the tumor. We use platinum needles because these are resistant to erosion and have high electric conductivity. The diameter of the needles is 0.07 cm and length 15 cm, values that justify why we assume in this mathematical approach that the electrode cross section is neglected respect to its length [Jiménez et al., 2011]. Saline solution and bleomycin are intratumor injected before and immediately after direct current application, respectively. It is made with the aim to potentiate the electrotherapy antitumor effectiveness, fact that is theoretically verified when the tumor conductivity increases with respect to that of the surrounding healthy tissue because the electric current density lines mainly distribute inside tumor and its periphery.

We observe that as soon as direct current is connected to the electrodes, different electrochemical reactions influence the pH-value and can cause electrolysis of tumor tissue, which in turn, lead to the destruction of it. The tumor regression induced by this electrodes array is approximately 50 % one month after the application of this therapy. Minima adverse effects (events) are observed after direct current application, probably due to that the electrodes are inside tumor and this therapy is local. We are not observed immediate adverse events (first 24 hours after electrotherapy is applied); however, we have reported late adverse events (after 24 hours of applied electrotherapy), such as: necrosis on the ulcerated surface, erythema and slight edema at the area treated, inflammation because the cancerous tissue is being destroyed through this method of treatment. Immediately after treatment, we do not observe pain, fever, superinfections. The destroyed cancerous tissue is eliminated from the body and is replaced by scar tissue and then in the majority of the patients, we observe tissue granulation when the tumor is removed after this treatment [Jarque et al., 2007]. Similar results are reported in laboratory animal [Cabrales et al., 2001; Ciria et al., 2004; Haltiwanger, 2008; Mikhailovskaya et al., 2009; Sazgarnia et al., 2009; Vijh, 2006] and human [Arsov et al., 2009; Haltiwanger, 2008; Jarque et al., 2007; Li et al., 2006; Salzberg et al., 2008; Vijh, 2006; Vogl et al., 2007; Xin et al., 2004; Yoon et al., 2007].

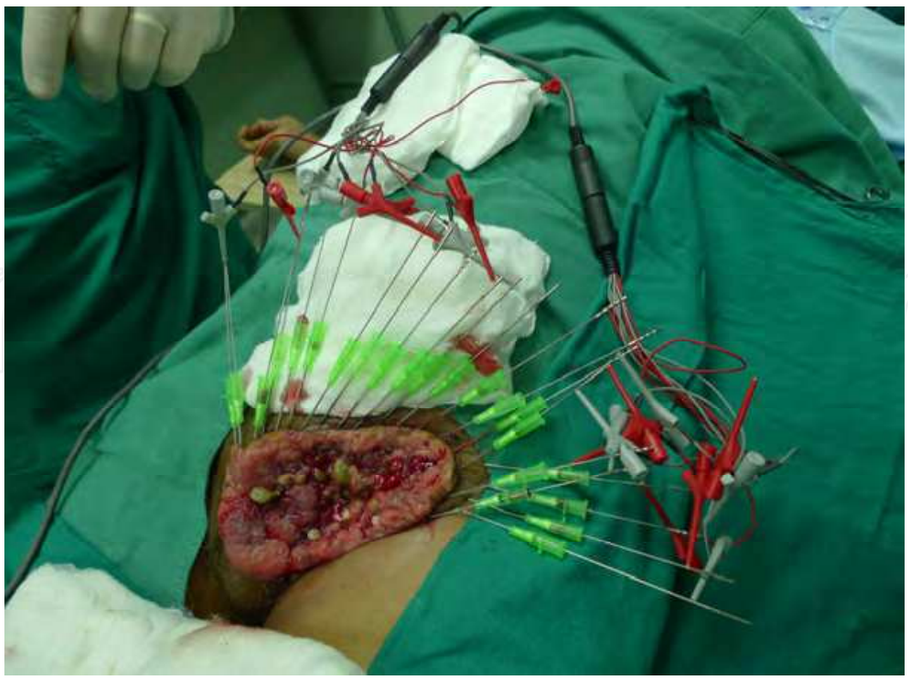

Fig. 9. Patient with vulva cancer treated with electrotherapy.

The use of this electrodes array stops the bloody flux of this patient for the vulva immediately after the electrotherapy application due to the haemostatic effect of the cathode. This fact may be explained because the cathode produces a tissue desiccation and therefore a control of the hemorrhage, in agreement with other results that demonstrate that the tumor blood flow is reduced by direct current action, fact that can be exploited to improve therapeutic outcome. It is well known that reductions in tumor blood flow can lead to an increase in hypoxia and extracellular acidification and as a result a cascade of tumor cell death will occur, due to a lack of nutrients, oxygen and an accumulation of catabolite products [Griffin et al., 1994; Haltiwanger, 2008; Xin et al., 2004]. As a result of this, this patient does not receive more blood transfusions post-treatment. This patient dies one year after the electrotherapy application due to multiple metastases in brain, lung and liver.

In electrotherapy, the electrodes are generally inserted outside of the central plane [Cabrales et al., 2001; Cabrales et al., 2010; Ciria et al., 2004; Chou et al., 1997; Jarque et al., 2007; Ren et al., 2001; Turler et al., 2000], constituting a limitation of the use of this radial electrodes array. This mathematical theorem solves the Problem 1 from the Problem 0 both harder and elastic needles. The solution of this problem becomes difficult in dependence on the complexity of this parametric form of the curve since more arduous is to solve the integral that appears in Equation (7). The simulations clearly demonstrate that analytical model is reliable and useful to search new electrode arrays that induce the highest electrotherapy effectiveness. New 3D-mathematical formalisms are obtained in dependence of the parametric curve form (Equation 3), which allow the insertion of the electrodes (hard or flexible) in any place of the tumor with arbitrary shape. This leads to solve problems more complex than that shown in a previous study [Jiménez et al., 2011] and to compare their electric current densities with those generated by other electrode arrays [Cabrales et al., 2001; Ciria et al., 2004; Chou et al., 1997; Jarque et al., 2007; Jiménez et al., 2011; Joa, 2010; Xin et al., 2004; Yoon et al., 2007].

Different authors report that there is a good correlation between the electric current density spatial distributions observed with different imaging techniques, those obtained by means of analytical and numerical solutions and experimental results [Miklavčič et al., 1998; Serša et al., 1997]. Among these techniques may be mentioned the Electric Current Density Imaging [Halter et al., 2007; Serša et al., 1997], Electrical Impedance Tomography [Saulnier et al., 2001], Magnetic Resonance Electrical Impedance Tomography [Seo et al., 2005], Magnetic Induction Tomography, Magnetoacoustic Tomography and Magnetoacoustic Tomography with Magnetic induction [Li et al., 2007]. These imaging techniques are useful to map spatial distribution of electric currents generated for any electrodes array in the tumor and its surrounding healthy tissue and to visualize the changes on electric current density patterns when the electrodes array parameters above mentioned are modified. These imaging techniques provide information on electrical conductivity inside an electrically conducting domain such as the human body and evidence that electric current density strongly depends on the placing, polarity and geometry of the electrodes, in agreement with our simulations. The quantification of the differences between the electric current densities obtained theoretically and experimentally is possible by means of an element average error (e) that can be evaluated by computing the integral over the element of the difference between the current density determined directly from the analytical expression (J_a) and the nodally averaged (interpolated) current densities over the region of support V_S (J_s), given by $e = \int_{V_S} (j_a - j_s) dV$. For this, it should be used the information provided by neighboring nodes to evaluate the magnitude of the higher order terms in the solutions that have been neglected.

These facts indicate that these imaging techniques may be used to know as change the electrical conductivity and current density distribution before, during and after electrotherapy. As a result of this fact, we have an idea of the structural, functional and pathological conditions of the tissue and therefore provide valuable diagnostic information. For this reason, we include in the electric current density the information of the electrical conductivities of the tumor and surrounding healthy tissue, whose mean values may be measured by means of such imaging techniques above mentioned [Li et al., 2007; Saulnier et al., 2001; Halter et al., 2007; Seo et al., 2005; Serša et al., 1997]. This justifies why the bulk conductivities of both tissues are assumed constant in our mathematical approach. The bulk electrical conductivity values of heterogeneous and anisotropic tissues may also be calculated, with good approximation, by means of their electric conductivity tensor mean values [Sekino et al., 2009]. We believe that the higher electric conductivity of the tumor is along of the preferential direction of growth (major diameter of tumor with ellipsoidal shape); however, an experiment should be designed to demonstrate this hypothesis. Although the majority of the solid tumors are heterogeneous, all are homogeneous for volumes ≤ 3 cm^3. Also, there are very few types of tumors (adenomas, adenocarcinomas, breast ductal carcinomas and sarcomas) with volumes > 3 cm^3 that are homogeneous, fact explained because is only observed tumor mass due to the equilibrium between the growth and the tumor cells angiogenesis. When this equilibrium is broken, the tumors make more heterogeneous due to the presence of necrosis, infiltration to tissues, among other alterations.

The fact that tumor conductivity is assumed higher than that its surrounding healthy tissue is justified because neoplasic tissues exhibit somewhat larger conductivity and permittivity values than homologous normal tissues due to that the water content is higher in the tumor

[Foster & Schwan, 1996; Haemmerich et al., 2003; Haemmerich et al., 2009; Miklavčič et al., 2006; Ng et al., 2008; S.R. Smith et al., 1986, D.G. Smith et al., 2000]. We believe that the presence of other charged particles (molecules, ions and electrons) and blood vessels (due to the angiogenic process) may also increase the tumor conductivity and therefore more current flows for the tumor, as we corroborate with the simulations shown in this chapter. These simulations have not included the effects that produce the direct current application on the tumor electric conductivity (permittivity); however, it should change during and after electrotherapy application. This may be due to that in the tumor are induced changes in the ions concentration in the intracellular and extracellular fluids [Griffin et al., 1994], structure and cellular density [Vijh, 2006; Von Euler et al., 2003], molecular composition [Von Euler et al., 2003], in the cellular membrane [Vodovnik et al., 1992; Yoon et al., 2007], among others. For instance, it has been demonstrated that the tumor conductivity changes before and after of the tumor thermal ablation [Haemmerich et al., 2009]. The changes of the electric conductivity may be one of the indicators of tissues conditions (anatomical and functional) [Seo et al., 2005]. We believe that for electric current densities (electric field intensities) below the reversible threshold value should not change significantly the tumor conductivity, not occurring thus above this threshold. This may be in correspondence with the tumor re-grow observed for $i/i_o < 2$ and the stationary partial and complete responses for $i/i_o \geq 2$, as shown in Figures 1 and 2 [Cabrales et al., 2008]. Hence, a detailed study should be carried out to know the explicit dependence between the electrical conductivity and the physiological parameters of the tumor. This may be used to establish an index for the prediction of the possible evolution of the patient during and after the direct current application (alone or combined). Also, an improved understanding of the theoretical basis of this dependence will enable structural features of the tumor tissue to be deduced from the experimental measurements.

Although it is assumed that the fields and charges are non-time varying, and the magnetic field due to the current and the reaction of this field on the current, we do not discard that magnetic field due to the direct current intensity produce bioeffects in the tumor, mainly around electrodes, in agreement with other authors [Saulnier et al., 2001; Seo et al., 2005]. It is possible that this induced magnetic field induces mechanical forces and shear stresses in the tumor that in dependence of its strength and duration may also produce a wide variety of biological effects in cells and tumor tissue, such as: electrodiffusion/osmosis (various receptors, charged membrane molecules, can be transported along the cell surface) and change in transmembrane potential (voltage-gated channels may be opened to permit the transport of ions, such as calcium, into the cell) [Hart, 2008].

It is important to point out that the images obtained with these experimental techniques are important because reveal that the spatial distribution of electric currents do not depends only on electrode array but, also on their tissue contact, which is hard to control [Foster, 1995; Serša et al., 1997]. The interaction electrode-tumor is not considered; however, it may have an important role in the skin heating. This heating is determined both by palpation with the hand and skin erythema of the patients with tumors treated with direct current [Jarque et al., 2007]. The tissue near of electrodes is heated mainly by the absorbed electrical energy, while regions further away may be heated by thermal conduction and/or some biophysic (electrochemical processes) induced into the tumor. As a consequence, the preferential heating of the tumor is governed by the electrical parameters near the electrode, whereas thermal parameters become increasingly important further away. An analysis of the energy (heat) absorbed by the tumor and its surrounding healthy tissue may be another

way to select these optima parameters. The absorbed energy can be calculated by means of the expression $Q_{1,2} = \int (j_{1,2}^2 / \sigma_{1,2}) dV$, where Q, j and σ are the absorbed heat quantity, electric current density and electric conductivity in the medium, respectively. The sub-indexes 1 and 2 represent to the medium 1 (tumor) and medium 2 (surrounding healthy tissue). Similar analyses of the absorbed energy quantity are carried out in radiotherapy and hyperthermia [Hall, 1988; Sadadcharam et al., 2008; Schaefer et al., 2008]. On the other hand, as the difference in electrical parameters between the tumor and its surrounding healthy tissue is substantial that might result in preferential heating of the tumor. This healing in dependence of its duration and intensity may be a result of the increase of the intratumor temperature that may provoke changes either directly or indirectly in the tissue dielectric properties and therefore irreversible damages in it [Foster, 1995]. The temperature dependence of the electrical conductivity may be related with damages in the tumor. In order to correctly mimic the absorbed energy in the tumor and its surrounding healthy tissue during electrotherapy exposure, a three dimensional model must be used.

Model tumor system as a spheroid is assumed for the following reasons: 1) the spheroid system has been applied to a number of problems in cancer and it is a model of a solid tumor in vitro and in vivo. 2) This system mimics many of these tumor characteristics and provides a rapid, useful, and economical method for screening sensitizers and chemotherapeutic agents because it is intermediate in complexity between single-cell in vitro culture and tumors in experimental animals. 3) The spheroid system is simpler, more reproducible, more economical, and easier to manipulate than animal tumors, and yet the cells can be studied in an environment that includes the complexities of cell-to-cell contact and nutritional stress from diffusion limitations that are characteristic of a growing tumor. 4) Some cells, notably several rodent tumor cell lines, such as chinese hamster V79 lung cells, mouse EMT6 mammary and R1F fibrosarcma cells, and rat 9L brain tumor cells grow as spheroids. At each successive division the daughter cells stick together, and the result is a spherical clump of cells that grows bigger and bigger with time. 5) Many types of human tumor cells can be cultured as spheroids with a wide spectrum of morphological appearance and growth rates. 6) Human tumor cell spheroids maintain many characteristics of the original tumor from the patient or of the some cells grown as xenografts. Human tumors successfully grown as spheroids include thyroid cancer, renal cancer, squamous carcinoma, colon carcinoma, neuroblastoma, human lung cancer, glioma, lymphoid tumors, melanoma, and osteosarcoma [Hall, 1988].

A feasible way to optimize 3D-electrode arrays is combining all the electrodes array parameters such that the electric current density in the tumor is the permissible maximum and that induced in the surrounding healthy tissue is smaller than 10 mA/m². For this, we suggest the following procedure: first, the parameters are automatically selected so that the electric current density in the surrounding healthy tissue is smaller than 10 mA/m². This guarantees the safety of the electrotherapy (Phase I of a Clinical Trial) and that the adverse effects in the organism are minima (Phase II of a Clinical Trial). Second, the selection of the optimum parameters depends on the electric current density (electric field strength) that induces the biggest tumor destruction (Phase III of a Clinical Trial), which may be experimentally verified by means of an experiment, in which is obtained the higher electrotherapy antitumor effectiveness, the maximum survival and life quality of the patient (laboratory animal). It evaluates the contributions of each parameter (alone or combined with other) and requires a significant consumption of calculation time for the parameters

quantity involved in these equations. For the implementation of this way, we should take into account that exposure of a biological cell to electric current density (electric field) can lead to a variety of biochemical and physiological responses. For this, it is required to know what electric current density values provoke significant biological effects: below 1 mA/m^2 (there are not biological effects); 1-10 mA/m^2 (minimum biological effects, which are not significant); 10-100 mA/m^2 (possible biological effects without risk to the health); 100-1000 mA/m^2 (biological effects without possible risk to the health) and above 1000 mA/m^2 (biological effects with proven risks to health) [International Commission on Non-Ionizing Radiation Protection, 1998]. This is very important because the electrotherapy effectiveness is highly depend on the magnitude and spatial distribution of electric currents flowing through the tumor and its surrounding healthy tissue, in agreement with other authors [Serša et al., 1997].

The knowledge of the optimum distributions of current density vector in the tumor and its surrounding healthy tissue allows the optimum design of noninvasive electromagnetic techniques for the cancer treatment. Several authors report that the ultralow-frequency extremely weak alternating component of combined magnetic fields exhibits a marked antitumor activity [Novikov et al., 2009]. These fields will avoid the insertion of electrodes in the tumor and therefore the little trauma that this provoke in the patients treated with electrotherapy. Weak magnetic fields activate the system of antitumor immunity (i.e., production of Tumor Necrosis Factor, activation of macrophages, among other) and produce reactive oxygen species, as is also observed on electrotherapy [Cabrales et al., 2001; Serša et al., 1994; Serša et al., 1996; Watemberg et al., 2008].

Different authors have experimentally evaluated the influence of direct current intensity [Ciria et al., 2004; Cabrales et al., 2010; Chou et al., 1997, Ren et al., 2001; Xing et al., 2004] and electromagnetic field [Novikov et al., 2009] on tumor growth kinetic; however, the weight of the different parameters of an electrodes array in it has not been widely discussed. Consequently, it is possible to simultaneously know, previous treatment, the possible tumor evolution in the time and the electric current density (potential, electric field intensity) distributions in the tumor and its surrounding healthy tissue and therefore the highest electrotherapy antitumor effectiveness. This improving therapy may be obtained when the tumor reaches its complete cure (complete remission or stationary partial response) [Cabrales et al., 2008; Cabrales et al., 2010] or the higher tumor growth delay (highest survival of the patients with good life quality and/or bigger disease free interval) [Ciria et al., 2004; Chou et al., 1997; Jarque et al., 2007; Ren et al., 2001; Xin et al., 2004; Yoon et al., 2007]. The evaluation of it requires to quantify different biological parameters, such as: tumor regression percentage, mean doubling time, survival rate, antibody responses, cellular responses, apoptosis, necrosis, histological examination, immune responses, and gene expressions, among others. This will contribute to elucidate the direct current antitumor mechanism.

The tumor complete response suggests that its growth kinetic is completely reversible, as shown in Figure 10 for fibrosarcoma Sa-37 tumor [Cabrales et al., 2010]. This behaviour is obtained from the experimental data [Ciria et al., 2004] and the analysis of the first and second parts of the tumor growth kinetic by means of the use of the modified Gompertz equation [Cabrales et al., 2010]. The first part comprehends the time that elapses from the initial moment at which tumor cells are inoculated in the host (t = 0 days) up to 15 days that is the moment of direct current application, when the tumor volume reaches $V_o = 0.5\ cm^3$), whereas the second part is the time that elapses from V_o up to the end of the experiment,

that is, time after direct current application. Both parts are obtained using the interpolation process and the time step is $\Delta t = 1/3$ days. The parameters i, α, β, γ and i_o are above defined and obtained from fitting the experimental data [Cabrales et al., 2008]. The analysis of these two parts reveals the existence of two tumor volumes that suggests the unavoidable tumor destruction: in the first, the tumor does not return to its state before direct current treatment, V_{id}, and therefore complete (stationary partial) response is reached. In the second, the small fraction tumor that survives to direct current action is completely destroyed by the organism, V_d, aspect that may suggest that the therapies for the cancer, including the electrotherapy, should be directed to that the tumor always reaches V_d. New investigations have been derived starting from this hypothesis.

In the case that complete remission (stationary partial response) of tumor is not reached after alone direct current stimulus, the electrotherapy should be directed to increase the survival and quality of life of patients (laboratory animals). First this, we should know the exact time in that electrotherapy may be repeated (time for which the tumor volume is between V_o and the minimum volume observed in tumor growth, V_{min}), as shown in Figure 11 [Cabrales et al., 2010]. When the tumor volume reaches this value there is a change of both slope and sign of the first derivate of the tumor volume (corresponding to minimum value of this first derivate), aspect that may indicate a tumor response (reorganization and/or activation of the growth and protection mechanisms) to the direct current action, whose intensity is not adequate to significantly perturb to it. This fact may be explained because the biological systems, as the tumors, respond to the external perturbations in order to reach their maxima survival. As a result, the electrotherapy should be repeated or combined with other therapies when the first derivate of the tumor volume changes of slope and sign because the tumor cannot be reorganized, in agreement with the current tendency of repeating weekly (every fifteen days) this therapy of 2 to 4 times. This constitutes a novel statement because establishes that this therapy should not be applied when the tumor volume reaches V_{min}, as is implemented for the treatment of patients at present [Jarque et al., 2007; Xin et al., 2004]. It is possible a fractionated therapy may lead to the complete (stationary partial) remission.

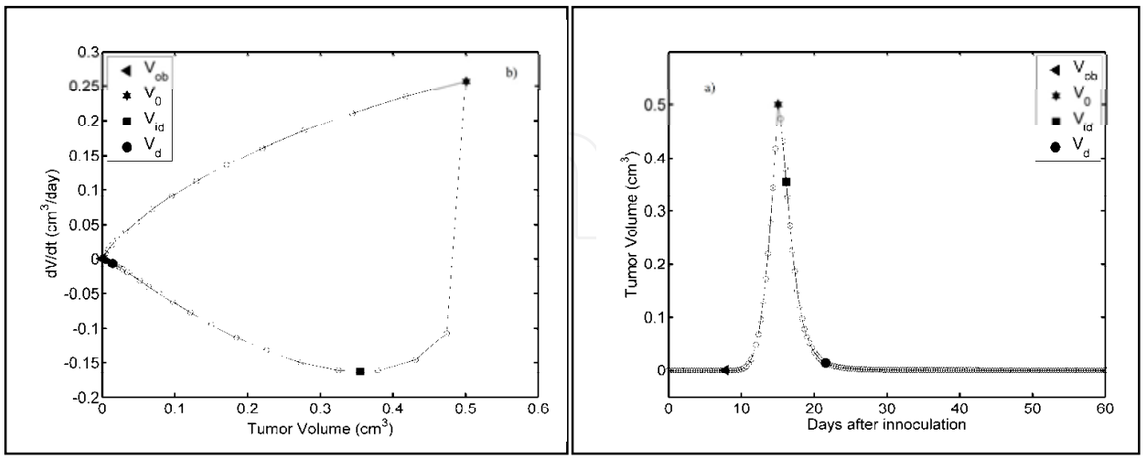

Fig. 10. Direct current-perturbed fibrosarcoma Sa-37 tumor growth kinetic for the parameters: $V_o = 0.5$ cm^3, i = 14.8 mA, $\alpha = 0.006$ days^{-1}, $\beta = 0.207$ days^{-1}, $\gamma = 0.189$ days^{-1}, $i_o = 1.080$ mA and $\Delta t = 1/3$ days. Time dependence of tumor volume (left picture). First derivate of tumor volume versus tumor volume (right picture).

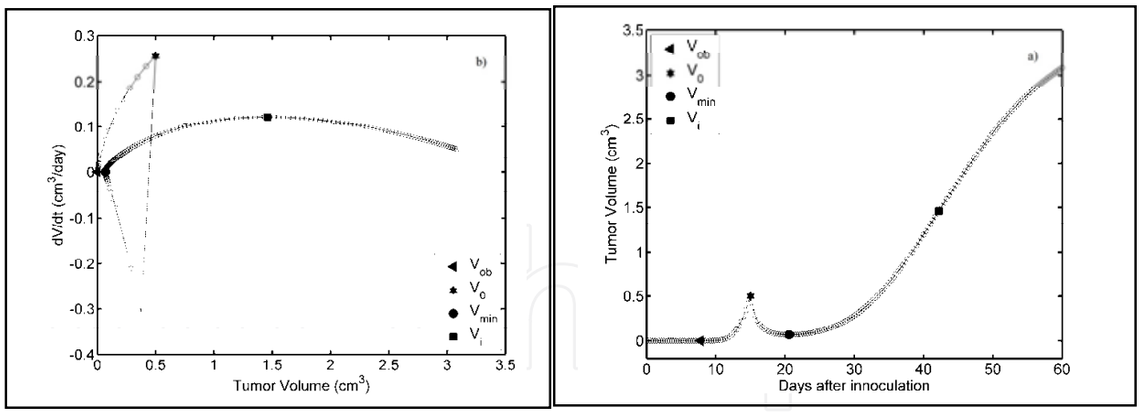

Fig. 11. Direct current-perturbed fibrosarcoma Sa-37 tumor growth kinetic for the parameters: V_o = 0.5 cm^3, i = 11.7 mA, α = 1.584 $days^{-1}$, β = 0.076 $days^{-1}$, γ = 0.107 $days^{-1}$, i_o = 7.431 mA and Δt = 1/3 days. Time dependence of tumor volume (left picture). First derivate of tumor volume versus tumor volume (right picture).

The inclusion of the other electrodes array parameters, in addition to direct current intensity, in the tumor growth kinetic may efficiently lead to complete (stationary partial) response for smaller direct current intensities.

The knowledge of these two parts of the tumor growth kinetic is important to reveal further information of it and in the therapeutic planning, as is widely discussed in a previous study. Similar results for fibrosarcoma Sa-37 tumor are also found Ehrlich tumor (results not shown) [Cabrales et al., 2010].

By optimizing the electrodes array parameters and those of the tumor growth kinetic (for instance, modified Gompertz equation), the efficiency of electrotherapy might be improved further. This procedure will have to be tested in larger animals to assess the usefulness and safety of electrotherapy in vivo for the future application to humans.

In spite of the considerable progress of electrotherapy, a number of challenges remain for the future. The future strategies include (a) increasing the volume of destroyed tissue at a single treatment session (b) the integration of electrotherapy with the other in-site tumor antitumor techniques and (c) the necessity of to incorporate realistic geometric, conductivity, and, eventually anisotropic information in order to reach the highest electrotherapy effectiveness.

3. Conclusion

In conclusion, electrotherapy of low-level direct current is promissory for cancer treatment. The electric current density (potential and electric field strength) analysis results can be used for assessing effective treatment parameters of tumor. The use of this mathematical approach and the theorem provide a rapid way to propose different optimum electrode arrays in dependence of location, depth, shape and size of the solid tumors with the purpose of obtaining the higher antitumor effectiveness and as a result to implement the electrotherapy in the Clinical Oncology.

4. Acknowledgements

This research is partially supported by the Ministry of Superior Education, Republic of Cuba. Also, the authors wish to thank to Ph.D. Carl Firley, Ph.D. Jesús Manuel Bergues Cabrales,

Ph.D. Juan José Godina Navas, MSc. Andrés Ramírez Aguilera, Bachelor Javier González Joa, Ph.D. Juan Bory Reyes, Bachelor Emilio Suárez, Ph.D. Francisco Martínez, Ph.D. Héctor Manuel Camué Ciria, MSc. Maraelys Morales González, M.D. Miguel Angel O´farril Mateus, M.D. Manuel Verdecia Jarque, M.D. Tamara Rubio González, MSc. Soraida Candida Acosta Brooks. M.D. María Cristina Céspedes Quevedo, M.D. Fabiola Suárez Palencia, M.D. Miriam Fariñas Salas, MSc. Lisset Ortíz Zamora and Ph.D. Gustavo Sierra González for their invaluable help and suggestions. Also, we thank in a special way the Editorial Board of this book, Ms Mia Devic and Ms. Masa Vidovic for the invitation to write this chapter.

5. References

Aguilera, A.R.; Cabrales, L.E.B.; Ciria, H.M.C.; Pérez, Y.S.; Oria, E.R. & Brooks, S.A. (2009). Distributions of the potential and electric field of an electrode elliptic array used in electrotherapy: Analytical and numerical solutions. *Mathematics and Computer in Simulation*, Vol.79, No.7, (March 2009), pp. 2091-2105, ISSN 0378-4754.

Aguilera, A.R.; Cabrales, L.E.B.; Ciria, H.M.C.; Pérez, Y.S.; González, F.G.; González, M.M.; Ortíz, L.Z.; Palencia, F.S.; Salas, M.F.; Bestard, N.R.; González, G.S. & Cabrales, I.B. (2010). Electric current density distribution in planar solid tumor and its surrounding healthy tissue generated by an electrode elliptic array used in electrotherapy. *Mathematics and Computer in Simulation*, Vol.80, No.9, (May 2010), pp. 1886-1902, ISSN 0378-4754.

Arsov, C.; Winter, C. & Albers, P. (2009). Value of galvanotherapy for localised prostate cancer. *Urologe*, Vol.48, No.7, (July 2009), pp. 748-754, ISSN 1433-0563.

Bellomo, N.; Li, N.K. & Maini, P.K. (2008). On the foundations of cancer modeling: selected topics, speculations, and perspectives. *Mathematical Models and Methods Applied Sciences*, Vol.18, No.4, (April 2008), pp. 593–646, ISSN 0218-2025.

Brú, A.; Albertos, S.; Subiza, J.L.; García-Asenjo, J.L. & Brú, I. (2003). The Universal Dynamics of Tumor Growth. *Biophysical Journal*, Vol.85, No.5, (November 2003), pp. 2948–2961, ISSN 0006-3495.

Cabrales, L.E.B.; Ciria, H.M.C.; Bruzón, R.N.P.; Quevedo, M.C.S.; Aldana, R.H.; González, L.M.O.; Salas, M.F. & Peña, O.G. (2001). Electrochemical treatment of mouse Ehrlich tumor with direct electric current: Possible role of reactive oxygen species and antitumoral defense mechanisms. *Bioelectromagnetics*, Vol.22, No.5, (July 2001), pp. 316-322, ISSN 0197-8462.

Cabrales, L.E.B.; Aguilera, A.R.; Jiménez, R.P.; Jarque, M.V.; Ciria, H.M.C.; Reyes, J.B.; Mateus, M.A.F.; Palencia, F.S. & Ávila, M.G. (2008). Mathematical modeling of tumor growth in mice following low-level direct electric current. *Mathematics and Computers in Simulation,* Vol.78, No.1, (June 2008), pp. 112-120, ISSN 0378-4754.

Cabrales, L.E.B.; Nava, J.J.; Aguilera, A.R.; Joa, J.A.G.; Ciria, H.M.C.; González, M.M., Salas, M.F.; Jarque, M.V.; González, T.R.; Mateus, M.A.F.; Brooks, S.C.A.; Palencia, F.S.; Zamora, L.O.; Quevedo, M.C.C.; Seringe, S.E.; Cutié, E.S.; Cabrales, I.B. & González, G.S. (2010). Modified Gompertz equation for electrotherapy murine tumor growth kinetics: predictions and new hypotheses. *BMC Cancer*, Vol.10, No.589, (October 2010), pp. 1-14, ISSN 1471-2407.

Ciria, H.M.C.; Quevedo, M.C.S.; Cabrales, L.E.B.; Bruzón, R.N.P.; Salas, M.F.; Peña, O.G.; González, T.R.; López, D.S. & Flores, J.L.M. (2004). Antitumor effectiveness of different amounts of electrical charge in Ehrlich and fibrosarcoma Sa-37 tumors. *BMC Cancer*, Vol.4, No.87, (November 2004), pp. 1-10, ISSN 1471-2407.

Chou, C.K.; McDougall, J.A.; Ahn, C. & Vora, N. (1997). Electrochemical Treatment of Mouse and Rat Fibrosarcomas with Direct Current. *Bioelectromagnetics*, Vol.18, No.1, (December 1997), pp. 14-24, ISSN 0197-8462.

Chou, C. (2007). Thirty-five years in bioelectromagnetics research. *Bioelectromagnetics*, Vol.28, No.3, (April 2007), pp. 3–15, ISSN 0197-8462.

Cohen, S.M. & Arnold, L.L. (2008). Cell Proliferation and Carcinogenesis. *Journal of Toxicology Pathology*, Vol.21, No.1, (April 2008), pp. 1-7, ISSN 0914-9198.

Čorović, S.; Pavlin, M. & Miklavčič, D. (2007). Analytical and numerical quantification and comparison of the local electric field in the tissue for different electrode configurations. *Biomedical Engineering Online, Vol.*6, No.1, (October 2007), pp. 37-50, ISSN 1475-925X.

Dev, B.S.; Dhar, D. & Krassowska, W. (2003). Electric field of a six-needle array electrode used in drug and DNA delivery in vivo: analytical versus numerical solution. *IEEE Transaction Biomedical Engineering*, Vol.50, No.11, (November 2003), pp. 1296-1300, ISSN 0018-9294.

Foster, K.R. & Schwan, H.P. (1996). Dielectric properties of tissues, In: *Handbook of Biological Effects of Electromagnetic Fields*, C. Polk & E. Postow (Ed.), 68–70 (Chapter 1), CRC Press LLC, ISBN 0-8493-06418, Boca Raton, Florida, USA.

Foster, K.R. (2000). Dielectric properties of tissues, In: *The Biomedical Engineering Handbook*, J.D. Bronzino, (Ed.), 1385-1394 (Chapter 89), CRC Press LLC, ISBN 0-8493-0461-X, Boca Raton, Florida, USA.

Griffin, D.T.; Dodd, N.F.J.; Moore, J.V.; Pullan, B.R. & Taylor, T.V. (1994). The effects of low level direct current therapy on a preclinical mammary carcinoma: tumor regression and systemic biochemical sequelae. *British Journal Cancer*, Vol.69, No.5, (May 1994), pp. 875-878, ISSN 0007-0920.

Haemmerich, D.; Staelin, S.T.; Tsai, J.Z.; Tungjitkusolmun, S.; Mahvi1, D.M. & Webster, J.G. (2003). *In vivo* electrical conductivity of hepatic tumours. *Physiological Measurement*, Vol.24, No.2, (February, 2003), pp. 251-260, ISSN 0967-3334.

Haemmerich, D.; Schutt, D.J.; Wright, A.W. & Webster, J.G. (2009). Electrical conductivity measurement of excised human metastatic liver tumors before and after thermal ablation. *Physiological Measurement*, Vol.30, No.5, (May 2009), pp. 459-466, ISSN 0967-3334.

Hall, E.J. (1988). *Radiobiology for the radiologist*, In J.B. Lippincott Company/Philadelphia, ISBN 0-397-50848-4, New York, USA.

Halter, R.J.; Hartov, A.; Heaney, J.A.; Paulsen, K.D. & Schned, A.R. (2007). Electrical impedance spectroscopy of the human prostate. *IEEE Transaction Biomedical Engineering*, Vol.54, No.7, (July 2007), pp. 1321-1327, ISSN 0018-9294.

Haltiwanger, S. (April 2008). The electrical properties of cancer cells, In: *Wind Power, 17.06.2010*, Available from http://www.royalrife.com (http://www.royalrife.com/haltiwanger1.pdf).

Hart, F.X. (2008). The mechanical transduction of physiological strength electric fields. *Bioelectromagnetics*, Vol.29, No.6, (September 2008), pp. 447-455, ISSN 0197-8462.

ICNIRP. (1998). Guidelines for limiting exposure to time-varying electric, magnetic, and electromagnetic fields up to 300 GHz. International Commission on Non-Ionizing Radiation Protection). *Health Physics*, Vol.74, No.4, (April 1998), pp. 494–522, ISSN 0017-9078.

Jarque, M.V.; Mateus, M.A.O.; Jing-hong, L.; Cabrales, L.E.B.; Palencia, F.S.; Ciria, H.M.C.; Brooks, S.C.A. & Salas, M.F. (2007). Primeras experiencias clínicas en Cuba sobre el uso de la electroterapia en cuatro pacientes con tumores sólidos malignos superficiales. *Revista Electrónica MEDISAN*, Vol. 11, No.1, (January-March 2007), pp. 1-13, ISSN 1029-3019.

Jiang, Y. (2005). A Multiscale Model for Avascular Tumor Growth. *Biophysics Journal*, Vol.89, No.6, (December 2005), pp. 3884-3894, ISSN 0006-3495.

Jiménez, R.P.; Pupo, A.E.B.; Cabrales, J.M.B.; Joa, J.A.G.; Cabrales, L.E.B.; Nava, J.J.G.; Aguilera, A.R.; Mateus, M.A.O.; Jarque, M.V. & Brooks, S.C.A. (2011). 3D stationary electric current density in to spherical tumor treated with low direct current. *Bioelectromagnetics*, Vol. 32, No.2, (February 2011), pp. 120-130, ISSN 1521-186X.

Joa, J.A.G. (2010). Three-dimensional visualization of the electric current density in the tumor and its surrounding healthy tissue generated by an electrode arrays. Analytic solution. *Thesis of Bachelor in Physics*, University of Oriente, Faculty of Natural Science, Department of Physics.

Kotnik, T. & Miklavčič, D. (2006). Theoretical evaluation of voltage inducement on internal membranes of biological cells exposed to electric fields. *Biophysics Journal*, Vol.90, No.2, (January 2006), pp. 480-491, ISSN 0006-3495.

Krüger, H. & Menzel, M. (1996). Clifford analytic vector fields as models for plane electric currents, *Proceedings of the symposium on analytical and numerical methods in quaternionic and Clifford analysis*, pp. 101-111, ISBN-10: 3860120417 (ISBN-13: 978-3860120415), Seiffen, Germany, June 5-7, 1996.

Li, K.H.; Xin, Y.L.; Gu, Y.N.; Xu, B.L.; Fan, D.J. & Ni, B.F. (1997). Effects of Direct Current on Dog Liver: Possible Mechanisms for Tumor Electrochemical Treatment. *Bioelectromagnetics*, Vol.18, No.1, (December 1997), pp. 2-7, ISSN 0197-8462.

Li, J.; Xin, Y.; Zhang, W.; Liu, J. & Quan, K. (2006). Effect of electro-acupuncture in treating patients with lingual hemangioma. *Chinese Journal of Integrative Medicine*, Vol.12, No.2, (June 2006), pp. 146-149, ISSN 162-0415.

Li, X.; Xu, Y. & He, B. (2007). Imaging electrical impedance from acoustic measurements by means of magnetoacoustic tomography with magnetic induction (MAT-MI). *IEEE Transactions on Biomedical Engineering*, Vol.54, No.2, (February 2007), pp. 323-330, ISSN 0018-9294.

Lin, X.Z.; Jen, C.M.; Chou, C.K.; Chou, C.S.; Sung, M.J. & Chou, T.C. (2000). Saturated saline enhances the effect of electrochemical therapy. *Digestive Diseases and Sciences*, Vol. 45, No.3, (March 2000), pp. 509-514, ISSN 0163-2116.

Mikhailovskaya, A.A.; Kaplan, M.A.; Brodskij, R.A. & Bandurko, L.N. (2009). Evaluation of Antitumor Efficiency of Electrochemical Lysis on the Model of M-1 Sarcoma. *Bulletin of Experimental Biology and Medicine*, Vol.147, No.1, (November 2009), pp. 88-90, ISSN 0007-4888.

Miklavčič, D.; Jarm, T.; Karba, R. & Serša, G. (1995). Mathematical modelling of tumor growth in mice following electrotherapy and bleomycin treatment. *Mathematics and Computers in Simulation*, Vol.39, No.5-6, (November 1995), pp. 597-602, ISSN 0378-4754.

Miklavčič, D.; Beravs, K.; Šemrov, D.; Čemažar, M.; Demšar, F. & Serša, G. (1998). The importance of electric field distribution for effective in vivo electroporation of tissues. *Biophysical Journal*, Vol.74, No.5, (May 1998), pp. 2152-2158, ISSN 0006-3495.

Miklavčič, D.; Pavšelj, N. & Hart, F.X. (2006). Electric Properties of Tissues. In: *Wiley Encyclopedia of Biomedical Engineering* John Wiley & Sons, New York, USA.

Mohammadi, B.; Haghpanah, V. & Larijani, B. (2008). A stochastic model of tumor angiogenesis. *Computers in Biology and Medicine,* Vol.38, No.2, (October 2008), pp. 1007-1011, ISSN 0010-4825.

Ng, E.; Sree, S.; Ng, K. & Kaw, G. (2008). The Use of Tissue Electrical Characteristics for Breast Cancer Detection: A Perspective Review. *Technology in Cancer Research and Treatment*, Vol.7, No.4, (August 2008), pp. 295-308, ISSN 1533-0338.

Nilsson, E. & Fontes, E. (2001). Mathematical modelling of physicochemical reactions and transport processes occurring around a platinum cathode during the electrochemical treatment of tumors. *Bioelectrochemistry*, Vol.53, No.2, (March 2001), pp. 213-224, ISSN 1567-5394.

Novikov, V.V.; Novikov, G.V. & Fesenko, E.E. (2009). Effect of weak combined static and extremely low-frequency alternating magnetic fields on tumor growth in mice inoculated with the Ehrlich ascites carcinoma. *Bioelectromagnetics*, Vol.30, No.5, (March 2009), pp. 343-351, ISSN 0197-8462.

Olaiza, N.; Magliettia, F.; Suáreza, C.; Molinab, F.V.; Miklavčič, D.; Mir, L. & Marshall, G. (2010). Electrochemical treatment of tumors using a one-probe two-electrode device. *Electrochimica Acta*, Vol.55, No.20, (August 2010), pp. 6010-6014, ISSN 0013-4686.

Reberšek, M.; Čorović, S.; Serša, G. & Miklavčič, D. (2008). Electrode commutation sequence for honeycomb arrangement of electrodes in electrochemotherapy and corresponding electric field distribution. *Bioelectrochemestry*, Vol.74, No.1, (November 2008), pp. 26-31, ISSN 1567-5394.

Ren, R.L.; Vora, N.; Yang, F.; Longmate, J.; Wang, W.; Sun, H.; Li, J.R.; Weiss, L.; Staud, C.; McDougall, J.A. & Chou, C.K. (2001). Variations of dose and electrode spacing for rat breast cancer electrochemical treatment. *Bioelectromagnetics*, Vol.22, No.3, (April 2001), pp. 205-211, ISSN 0197-8462.

Sadadcharam, M.; Soden, D.M. & O'sullivan, G.C. (2008). Electrochemotherapy: An emerging cancer treatment. *International Journal of Hyperthermia*, Vol.24, No.3, (January 2008), pp. 263-273, ISSN 0265-6736.

Salzberg, M.; Kirson, E.; Palti, Y. & Rochlitza, C. (2008). A Pilot Study with Very Low-Intensity, Intermediate-Frequency Electric Fields in Patients with Locally Advanced and/or Metastatic Solid Tumors. *Onkologie*, Vol.31, No.7, (July 2008), pp. 362-365, ISSN 0378-584X.

Saulnier, G.J.; Blue, R.S.; Newell, J.C.; Isaacson, D. & Edic, P.M. (2001). Electrical impedance tomography. *IEEE Signal Processing Magazine*, Vol.18, No.6, (November 2001), pp. 31-43, ISSN 1053-5888.

Sazgarnia, A.; Bahreyni, T.S.; Shirin, S.M.; Bayani, R.S.; Khouei, A.L.; Esmaeili, H.E. & Homaei, F. (2009). Treatment of colon carcinoma tumors by electrolysis: effect of electrical dose and polarity. *Iranian Journal of Medical Physics*, Vol.5, No.2(20-21), (Winter 2009), pp. 39-51, ISSN 1735-160X.

Schaefer, N.; Schafer, H.; Maintz, D.; Wagner, M.; Overhaus, M.; Hoelscher, A.H. & Türler A. (2008). Efficacy of Direct Electrical Current Therapy and Laser-Induced Interstitial Thermotherapy in Local Treatment of Hepatic Colorectal Metastases: An Experimental Model in the Rat. *Journal of Surgical Research*, Vol.146, No.2, (May 2008), pp. 230-240, ISSN 0022-4804.

Sekino, M.; Ohsaki, H.; Yamaguchi-Sekino, S.; Iriguchi, N. & Ueno, S. (2009). Low-frequency conductivity tensor of rat brain tissues inferred from diffusion MRI. *Bioelectromagnetics*, Vol.30, No.6, (September 2009), pp. 489-499, ISSN 0197-8462.

Šel, D.; Mazeres, S.; Teissié, J. & Miklavčič, D. (2003). Finite-element modeling of needle electrodes in tissue from the perspective of frequent model computation. *IEEE Transaction Biomedical Engineering*, Vol.50, No.11, (November 2003), pp. 1221-1232, ISSN 0018-9294.

Seo, J.K.; Kwon, O. & Woo, E.J. (2005). Magnetic resonance electrical impedance tomography (MREIT): conductivity and current density imaging. *Journal of Physics: Conference Series*, Vol.12, No.1, (June 2004), pp. 140-155, ISSN 1742-6588.

Serša, G. & Miklavčič, D. (1990). Inhibition of Sa-1 tumor growth in mice by human leucocyte interferon alpha combined with low-level direct current. *Molecular Biotherapy*, Vol.2, No.3, (September 1990), pp. 165-168, ISSN 0952-8172.

Serša, G.; Miklavčič, D.; Batista, U.; Novakovič, S.; Bobanovič, F. & Vodovnik, L. (1992). Antitumor effect of electrotherapy alone or in combination with interleukin-2 in mice with sarcoma and melanoma tumors. *Anti-Cancer Drugs*, Vol.3, No.3, (June 1992), pp. 253-260, ISSN 0959-4973.

Serša, G.; Golouh, R. & Miklavčič, D. (1994). Antitumor effect of tumor necrosis factor combined with electrotherapy on mouse sarcoma. *Anti-Cancer Drugs*, Vol.5, No.1, (February 1994), pp. 69-74, ISSN 0959-4973.

Serša, G.; Kotnik, V.; Cemazar, M.; Miklavčič, D. & Kotnik, A. (1996). Electrochemotherapy with bleomycin in SA-1 tumor bearing mice-natural resistance and immune responsiveness. *Anti-Cancer Drugs*, Vol.7, No.7, (September 1996), pp. 785-791, ISSN 0959-4973.

Serša, I.; Beravs, K.; Dodd, N.J.F.; Zhao, S.; Miklavčič, D. & Demsar, F. (1997). Electric current density imaging of mice tumors. *Magnetic Resonance in Medicine*, Vol.37, No.3, (March 1997), pp. 404-409, ISSN 1522-2594.

Smith, S.R.; Foster, K.R. & Wolf, G.L. (1986). Dielectric properties of VX-2 carcinoma versus normal liver tissue. *IEEE Transaction Biomedical Engineering*, Vol.33, No.5, (May 1986), pp. 522-254, ISSN 0018-9294.

Smith, D.G.; Potter, S.R.; Lee, B.R.; Ko, W.W.; Drummond, W.R.; Telford, J.K. & Partin, A.W. (2000). In vivo measurement of tumor conductiveness with the magnetic bioimpedance method. *IEEE Transaction Biomedical Engineering*, Vol.47, No.10, (October 2000), pp. 1403-1405, ISSN 0018-9294.

Stein, W.D.; Figg, W.D.; Dahut, W.; Stein, A.D.; Hoshen, M.B.; Price, D.; Bates, S.E. & Fojo, T. (2008). Tumor Growth Rates Derived from Data for Patients in a Clinical Trial Correlate Strongly with Patient Survival: A Novel Strategy for Evaluation of Clinical Trial Data. *The Oncologist*, Vol.13, No.10, (October 2008), pp. 1046-1054, ISSN 1083-7159.

Turjanski, P.; Olaiz, N.; Abou-Adal, P.; Suarez, C.; Risk, M. & Marshall, G. (2009). pH front tracking in the electrochemical treatment (EChT) of tumors: Experiments and simulations. *Electrochimica Acta*, Vol.54, No.26, (November 2009), pp. 6199-6206, ISSN 0013-4686.

Turler, A.; Schaefer, H.; Schaefer, N.; Wagner, M.; Maintz, D.; Qiao, J.C. & Hoelscher, A.H. (2000). Experimental low-level direct current therapy in liver metastases: influence of polarity and current dose. *Bioelectromagnetics*, Vol.21, No.5, (July 2000), pp. 395-401, ISSN 0197-8462.

Veiga, V.F.; Nimrichter, L.; Teixeira, C.A.; Morales, M.M.; Alviano, C.S.; Rodrigues, M.L. & Holandino, C. (2005). Exposure of Human Leukemic Cells to Direct Electric

Current: Generation of Toxic Compounds Inducing Cell Death by Different Mechanisms. *Cell Biochemical Biophysics*, Vol.42, No.1, (February 2005), pp. 61-74, ISSN 1085-9195.

Vijh, A. (2004). Electrochemical treatment (ECT) of cancerous tumours: necrosis involving hydrogencavitation, chlorine bleaching, pH changes, electroosmosis. *International Journal of Hydrogen Energy*, Vol.29, No.6, (May 2004), pp. 663-665, ISSN 0360-3199.

Vijh, A.K. (2006). Phenomenology and Mechanisms of Electrochemical Treatment (ECT) of Tumors. In. *Modern Aspects of Electrochemistry*, C.G. Vayenas, R.E. White, M.E. Gamboa-Adelco (Ed.), 231-274 (Vol. 39), Springer, ISBN-10: 0-387-23371-7 (ISBN-13: 978-0387-23371-0, ISBN: 0-387-31701-5), New York, USA.

Vinageras, E.N.; de la Torre, A.; Rodríguez, M.O.; Ferrer, M.C.; Bravo, I.; del Pino, M.M.; Abreu, D.A.; Brooks, S.C.A.; Rives, R.; Carrillo, C.C.; Dueñas, M.G.; Viada, C.; Verdecia, B.G.; Ramos, T.C.; Marinello, G.G. & Dávila, A.L. (2008). Phase II Randomized Controlled Trial of an Epidermal Growth Factor Vaccine in Advanced Non–Small-Cell Lung Cancer. *Journal of Clinical Oncology*, Vol.26, No.9, (March 2008), pp. 1452-1458, ISSN 0732-183X.

Vodovnik, L.; Miklavčič, D. & Serša, G. (1992). Modified cell proliferation due to electrical currents. *Medical & Biological Engineering & Computing*, Vol.30, No.4, (July 1992), pp. CE21-CE28, ISSN 0140-0118.

Vogl, T.J.; Mayer, H.P.; Zangos, S.; Bayne, J.; Ackermann, H. & Mayer, F.B. (2007). Prostate Cancer: MR Imaging–guided Galvanotherapy-Technical Development and First Clinical Results. *Radiology*, Vol.245, No.3, (December 2007), pp. 895-902, ISSN 0033-8419.

Von Euler, H.; Olsson, J.M.; Hultenby, K.; Thorne, A. & Lagerstedt, A.S. (2003). Animal models for treatment of unresectable liver tumours: a histopathologic and ultra-structural study of cellular toxic changes after electrochemical treatment in rat and dog liver. *Bioelectrochemistry*, Vol.59, No.1-2, (April 2003), pp. 89-98, ISSN 1567-5394.

Wartenberg, M.; Wirtz, N.; Grob, A.; Niedermeier, W.; Hescheler, J.; Peters, S.C. & Sauer, H. (2008). Direct current electrical fields induce apoptosis in oral mucosa cancer cells by NADPH oxidase-derived reactive oxygen species. *Bioelectromagnetics*, Vol.29, No.1, (January 2008), pp. 47-54, ISSN 0197-8462.

Xiang, S.D.; Scalzo-Inguanti, K.; Minigo, G.; Park, A.; Hardy, C.L. & Plebanski, M. (2008). Promising particle-based vaccines in cancer therapy. *Expert Reviews of Vaccines*, Vol.7, No.7, (September 2008), pp. 1103-1119, ISSN 1476-0584.

Xin, Y.; Zhao, H.; Zhang,W.; Liang, C.; Wang, Z. & Liu, G. (2004). *Electrochemical Therapy of Tumors*, Bioelectromagnetic Medicine, Marcel Dekker Inc., ISBN 709-726, New York, USA.

Yen, Y.; Li, J.R.; Zhou, B.S.; Rojas, F.; Yu, J.; Chou, C.K. (1999). Electrochemical treatment of human KB cells in vitro. *Bioelectromagnetics*, Vol.20, No. 1, (January 1999), pp. 34-41, ISSN 0197-8462.

Yoon, D.S.; Ra, Y.M.; Ko, D.G.; Kim, Y.M.; Kim, K.W.; Lee, H.Y.; Xin, Y.L.; Zhang, W.; Li, Z.H. & Kwon, H.U. (2007). Introduction of Electrochemical Therapy (EChT) and Application of EChT to the breast Tumor. *Journal of Breast Cancer*, Vol.10, No.2, (June 2007), pp. 162-168, ISSN 1738-6756.

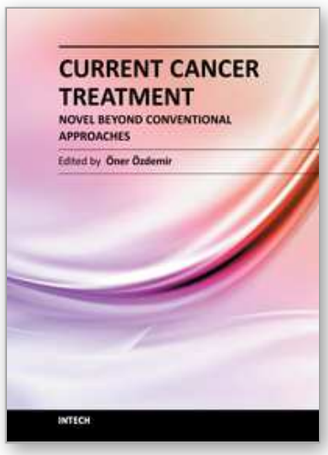

Current Cancer Treatment - Novel Beyond Conventional Approaches

Edited by Prof. Oner Ozdemir

ISBN 978-953-307-397-2
Hard cover, 810 pages
Publisher InTech
Published online 09, December, 2011
Published in print edition December, 2011

Currently there have been many armamentaria to be used in cancer treatment. This indeed indicates that the final treatment has not yet been found. It seems this will take a long period of time to achieve. Thus, cancer treatment in general still seems to need new and more effective approaches. The book "Current Cancer Treatment - Novel Beyond Conventional Approaches", consisting of 33 chapters, will help get us physicians as well as patients enlightened with new research and developments in this area. This book is a valuable contribution to this area mentioning various modalities in cancer treatment such as some rare classic treatment approaches: treatment of metastatic liver disease of colorectal origin, radiation treatment of skull and spine chordoma, changing the face of adjuvant therapy for early breast cancer; new therapeutic approaches of old techniques: laser-driven radiation therapy, laser photo-chemotherapy, new approaches targeting androgen receptor and many more emerging techniques.

How to reference

In order to correctly reference this scholarly work, feel free to copy and paste the following:

Ana Elisa Bergues Pupo, Rolando Placeres Jiménez and Luis Enrique Bergues Cabrales (2011). Electrotherapy on Cancer: Experiment and Mathematical Modeling, Current Cancer Treatment - Novel Beyond Conventional Approaches, Prof. Oner Ozdemir (Ed.), ISBN: 978-953-307-397-2, InTech, Available from: http://www.intechopen.com/books/current-cancer-treatment-novel-beyond-conventional-approaches/electrotherapy-on-cancer-experiment-and-mathematical-modeling

INTECH
open science | open minds

InTech Europe
University Campus STeP Ri
Slavka Krautzeka 83/A
51000 Rijeka, Croatia
Phone: +385 (51) 770 447
Fax: +385 (51) 686 166
www.intechopen.com

InTech China
Unit 405, Office Block, Hotel Equatorial Shanghai
No.65, Yan An Road (West), Shanghai, 200040, China
中国上海市延安西路65号上海国际贵都大饭店办公楼405单元
Phone: +86-21-62489820
Fax: +86-21-62489821

IntechOpen